University of Calgary

PRISM Repository **https://prism.ucalgary.ca**

The Vault Open Theses and Dissertations

2013-04-30

Comparisons of EmrE Purification Methods

Chew, Raymond

Chew, R. (2013). Comparisons of EmrE Purification Methods (Master's thesis, University of Calgary, Calgary, Canada). Retrieved from https://prism.ucalgary.ca. doi:10.11575/PRISM/25377 http://hdl.handle.net/11023/661

Downloaded from PRISM Repository, University of Calgary

UNIVERSITY OF CALGARY

Comparisons of EmrE Purification Methods

by

Raymond Chew

A THESIS

SUBMITTED TO THE FACULTY OF GRADUATE STUDIES

IN PARTIAL FULFILLMENT OF THE REQUIREMENTS FOR THE

DEGREE OF MASTER OF SCIENCE

DEPARTMENT OF BIOLOGICAL SCIENCES

CALGARY, ALBERTA

APRIL 2013

©Raymond Chew 2013

Acknowledgements

To my supervisor, Ray Turner, who was a great guide and mentor throughout my term in his lab. His patience, understanding, and optimism with science were contagious and influential.

To Jennifer Litzenberger, Simon Taylor, and Liana Houjeiri, who helped isolate untagged EmrE samples.

To all committee members for their ideas and advice during our meetings and gatherings.

To my family, Alex, Jacoba, and Phoebe, for all of their support and badminton to take my mind off science every once in a while.

To all members of the Turner lab, for all of the moral support during whiskey Wednesdays, karaoke nights, and intriguing off-topic conversations.

To Alex and Patrick, for all those work-out and wings nights that kept me physically fit, my appetite full, and renewed my perspective when I needed it.

To the band, Bennett, Sean, and Riley, for Thursday night jam sessions where awesome sounds were heard, instruments were played, and music was created.

Table of Contents

Chapter One: Introduction 6

1.1 INTEGRAL MEMBRANE PROTEINS 13

1.2 PROCESS OF INTEGRAL MEMBRANE PROTEIN INSERTION 16

1.3 MEMBRANE PROTEIN EXPRESSION TECHNOLOGIES 18

1.4 AFFINITY POLYHISTIDINE TAGGED-MEMBRANE PROTEIN FUSIONS 20

1.5 INTEGRAL MEMBRANE PROTEIN RECONSTITUTION 21

1.6 MEMBRANE PROTEIN ASSAYING CONDITIONS 22

1.7 MULTIDRUG RESISTANCE 23

1.8 BACTERIAL SMALL MULTIDRUG RESISTANCE PROTEINS 26

1.9 EMRE BIOCHEMISTRY 29

1.10 GOALS AND AIMS 32

Chapter Two: Materials and methods 33

2.1 STRAINS, PLASMIDS, AND MOLECULAR BIOLOGY 33
2.1.1 Untagged emrE 33
2.1.2 Tagged emrE 34

2.2 MUTAGENESIS TO GENERATE TAGGED EMRE 34

2.3 DOT BLOT ANALYSIS OF TAGGED EMRE PROTEIN ACCUMULATION IN *E. COLI* CULTURE 39

2.4 GROWTH CURVES OF *E. COLI* ACCUMULATING TAGGED EMRE 40

2.5 EMRE PURIFICATION PROCEDURES 40
2.5.1 Lysogeny broth 40
2.5.2 Accumulation of untagged EmrE in batch culture 40
2.5.3 Chloroform: methanol extraction and size-exclusion chromatography 42
2.5.4 Accumulation of tagged EmrE in batch culture 45
2.5.5 Immobilized nickel affinity chromatography 45
2.5.6 HiTrap desalting chromatography 48

2.6 SDS-TRICINE PAGE ANALYSIS....48

2.7 FLUORESCENCE....49

2.8 RED EDGE EXCITATION SHIFT SPECTRA COLLECTION....49

2.9 LIGAND BINDING....50
2.9.1 Fluorimeter parameters during ligand titration....51
2.9.2 Ligand and baseline signal considerations....51
2.9.3 Range-finding assays....51
2.9.4 Dilution effects and lamp intensity....52

2.10 RESISTANCE ASSAYS....55

Chapter Three: Protein purification....57

3.1 OPTIMIZING TAGGED EMRE PROTEIN ACCUMULATION IN BATCH CULTURE....57
3.1.1 Dot blot assays....57
3.1.2 Results....58
3.1.3 Growth curves....60
3.1.4 Results....60

3.2 SDS-TRICINE PAGE ANALYSIS OF PURIFIED EMRE....62
3.2.1 Results....62

3.3 EMRE SOLUBILISATION AND CONCENTRATION DETERMINATION....64
3.3.1 Protein concentration determination....65
3.3.2 Absorbance results....66
3.3.3 Identifying the source of light scattering....67
3.3.4 Discussion....70
3.3.5 Protein concentration determination by band intensities on a SDS-Tricine PAGE....70
3.3.6 Discussion....71

Chapter Four: Fluorescence Spectroscopy....73

4.1 FLUORESCENCE SPECTRA....73

4.2 RESULTS....74

4.3 DISCUSSION....76
Chapter Five: Red-edge excitation shift....77

5.1 THE REES EFFECT 77

5.2 RESULTS 79

5.3 DISCUSSION 82

Chapter Six: EmrE-Ligand binding 85

6.1 BACKGROUND 85

6.2 RESULTS 88
6.2.1 Baseline corrections 88
6.2.2 Calculations and plotting of ligand binding curves 90
6.2.3 Ligand binding 90

6.3 DISCUSSION 95

Chapter Seven: Resistance assays 99

7.1 BACKGROUND 99

7.2 RESULTS 101

7.3 DISCUSSION 103

Chapter Eight: Conclusions 106

Chapter Nine: Bibliography 110

Abbreviations and shorthand:

ATP – adenosine tri-phosphate. The energy currency in a cell.

B_{max} – a value representing the concentration for a ligand to saturate all binding sites

C43(DE3) – *Escherichia coli* strain used for accumulating tagged EmrE (in this study)

CMC – critical micelle concentration

CTPC –cetylpyridinium (chloride)

DDM – dodecyl maltoside

DNA – deoxy-ribonucleic acid

Eb – ethidium (bromide)

Empty vector – a plasmid that does not contain the gene of interest (emrE) in its multiple cloning site.

EmrE – *Escherichia coli* multidrug resistance E. An integral membrane protein.

FtsY – a signal recognition particle receptor homologue in prokaryotes.

Glu – glutamate, an amino acid

His_6 – a polyhistidine amino acid sequence of 6 histidine residues

HLB – hydrophilic – lipophilic balance

HRP – horse-radish peroxidase

IMP – integral membrane proteins

IPTG – isopropyl β-D-1-thiogalactopyranoside

ITC – isothermal titration calorimetry

K_d – dissociation constant

λ_{max} – wavelength representing the peak maximum (of an emission spectra)

lac promoter – a promoter that originally regulated lactose metabolism in bacteria. RNA polymerase binds this site to begin gene transcription.

lacI – name of gene encoding the *lac* promoter suppressor protein. The protein LacI binds the *lac* promoter preventing gene transcription.

*lac*UV5 promoter – a mutated version of the *lac* promoter that is less sensitive to cyclic AMP (a signalling molecule) levels within the cell.

LB – lysogeny broth

Leu – Leucine, an amino acid

LE392Δ*unc* – *Escherichia coli* strain used to accumulate untagged EmrE (in this study)

M – a unit of concentration, can also be represented as moles / L.

MV – methyl viologen (dichloride)

myc-His_6 – refers to the affinity tag of tagged EmrE (*myc* epitope sequence – linker – 6 histidine)

NAWA – *n*-acetyl-tryptophan amide

OD_{550} – optical density value. The subscript denotes the wavelength of light used for the optical density measurement (in this case, 550 nm).

PAGE – poly-acrylamide gel electrophoresis

QCC – quaternary cationic compounds

REES – red-edge excitation shift

RNA – ribonucleic acid

rotovap – rotary evaporator

Sec-dependent pathway – a specific translocation pathway for secreted proteins and inserted membrane proteins.

Sec-translocase – A multi-subunit membrane protein assembly that expends ATP to bring proteins across the lipid membrane.

SMR proteins – small multidrug resistance proteins

%T – percent total acrylamide used in an gel.

TCE – 2,2,2-trichloroethanol

TPP+ - tetraphenyl phosphonium, a QCC

Trp – tryptophan, an amino acid

Tyr – tyrosine, an amino acid

Val – Valine, an amino acid

YidC – A membrane protein that is involved in the insertion of other membrane proteins.

List of Tables:

2.1 Ligand binding titration order.....54

3.1 Yields of Untagged and Tagged EmrE from respective isolations 63

6.1 Binding affinities of QCC to EmrE evaluated under different conditions 86

6.2 Summary of EmrE-ligand binding values 91

List of Figures:

1.1 A generalized model of an alpha-helical membrane protein 5

1.2 Model of the Sec translocase system 17

1.3 Chemical structures of ethidium, methyl viologen, and cetylpyridinium 28

1.4 A comparison of the amino acid sequences of untagged and tagged EmrE 31

2.1 Plasmid maps of pEmr-11 and pTZEmrEmH6 36

2.2 Primers used for site-directed mutagenesis of the linker region of tagged EmrE 38

2.3 Size-exclusion chromatography elution profile for untagged EmrE purification 44

2.4A Immobilized metal affinity chromatography elution profile for tagged EmrE 47

2.4B HiTrap desalting chromatography elution profile for tagged EmrE 47

3.1 Dot blot analysis of tagged EmrE cultures 59

3.2 8 h growth curves of C43(DE3) cells containing the pEmrEmH6 plasmid or empty vector 61

3.3 SDS-Tricine PAGE of untagged and tagged EmrE from respective purifications 63

3.4 Absorbance spectra of untagged and tagged EmrE 69

3.5 Estimation of protein concentrations by SDS-Tricine PAGE band intensities 72

4.1 Fluorescence spectra of untagged and tagged EmrE 75

5.1 Jablonski diagram illustrating the REES effect 78

5.2 Emission spectra of untagged and tagged EmrE at different excitation wavelengths 80

5.3 Plot of emission maxima against excitation wavelength used (REES plot) 81

5.4 Jablonski diagram illustrating the reverse-relaxation phenomenon 84

6.1 Baseline emission spectra of Tris-based buffer containing DDM 89

6.2 Ligand binding curves of untagged and tagged EmrE to ethidium, methyl viologen, and cetylpyridinium 93

6.3 Deviations of ligand binding from the single-site specific binding model expressed as a residual plot 94

6.4 Hypothetical model of EmrE-QCC binding interactions 98

7.1 Hypothetical models of EmrE transport and effect of the fusion tag 100

7.2 26 h endpoint densities of cultures expressing untagged and tagged *emrE* under varying concentrations of ethidium or methyl viologen 102

Abstract:

Due to the difficulties of membrane protein expression, isolation, and solubilisation, purification yields are typically lower than most soluble proteins. A common tactic to increase yield is the use of affinity tags for co-purification of the attached protein. EmrE, a small bacterial multidrug efflux protein was examined to characterize changes in structure and function due to a His6 affinity tag. Fluorescence spectroscopy revealed the presence of a relatively hydrophobic fold in tagged EmrE as well as slower solvent dynamics within the folded protein. In regards to functionality, the untagged EmrE displayed higher ligand binding affinities to ethidium and methyl viologen in vitro and also higher transport activity in vivo.

Chapter One: **Introduction**

1.1 Integral membrane proteins

Biological membranes serve as barriers between the cell and the environment. The membrane itself is a complex structure that varies in composition between different organisms. Exchange of nutrients, synthesis of energy molecules, cell signalling are all processes that are facilitated through membranes with the assistance of associated proteins. Inhibition of membrane protein activity can lead to diseased states to lethality for the organism. In contrast to soluble proteins, all membrane proteins are embedded in the lipid bilayer or covalently bound to lipids in some way. The focus of this discussion will be on one type of membrane protein: the integral membrane protein (IMP). Integral membrane proteins are folded chains of polypeptides that insert into and span a lipid bilayer. Within cellular membranes, these proteins perform a variety of functions assisting the exchange of intra and extra-cellular materials, acting as sensors to environmental or chemical stimulus, facilitate in a signalling pathway, or modify bilayer components, including the folding and insertion of other membrane proteins. Currently, membrane protein characterization has been relatively limited in comparison to soluble proteins (White and Wimley, 1999). Integral membrane proteins have a transmembrane region which can either be a beta-sheet motif such as a beta-barrel, or an alpha helix. The larger beta-barrel structures are relatively less common and can usually be found in the outer membranes of Gram-negative bacteria. In contrast, 20-30% of all proteins are estimated to be alpha-helical integral membrane proteins (Wallin and von Heijne, 2008). An alpha helix contains approximately 3.6 residues per turn and a minimum of 20 amino

acids to span a typical lipid bilayer. Longer transmembrane helices possess a “tilt” as opposed to being perpendicular to the membrane. Non-polar or hydrophobic amino acid residues such as leucine, valine, and isoleucine, comprise the transmembrane region to reduce unfavorable interactions with hydrophobic lipid alkyl chains. Additional amino acid sequences form loop regions connecting different alpha helices or larger folded domains outside transmembrane regions can be present to carry out different enzymatic or regulatory functions. A hypothetical alpha helical IMP is shown in figure 1.1. As for the orientation of an IMP, a “positive inside rule” usually governs its topology. This rule states that the protein is orientated in such a way that most of the positive non-transmembrane residues face the cytoplasm (von Heijne, 1989).

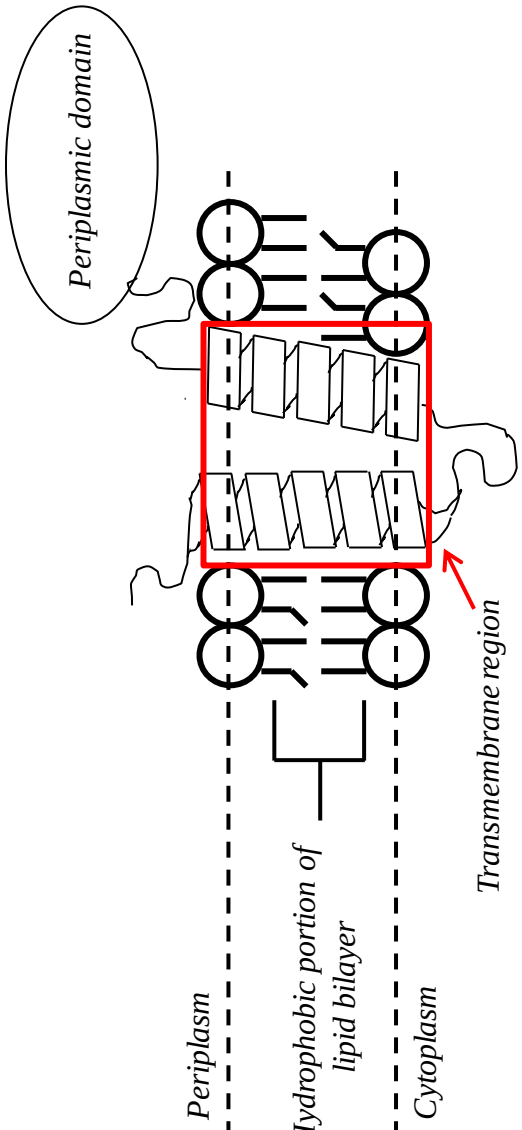

Figure 1.1: A hypothetical alpha-helical integral membrane protein in a gram-negative bacteria inner membrane. Typical components of a membrane protein are diagrammed: the traversing of the bilayer, possible folded regions extending beyond the transmembrane region, and loops linking transmembrane components.

1.2 Process of integral membrane protein insertion

Currently the number of possible insertional pathways is unknown and only a few have been well-characterized. Beta barrel pores that are found in the outer membranes of bacteria, mitochondria, and chloroplasts insert in a manner different from alpha-helical proteins that can be found on inner and plasma membranes. A review of beta-barrel insertion can be found here (Schleiff and Soll, 2005). As for alpha helical proteins, the sec-dependent pathway has been the subject of intensive work (Mori and Ito, 2001). In bacteria, insertion through this pathway is co-translational. First, a 14S signal recognition particle (SRP) composed of RNA can bind onto a polypeptide signal sequence emerging from ribosome and target the protein to a membrane receptor. In *E. coli*, the SRP-polypeptide-ribosome complex is targeted to an FtsY receptor and the complex can be passed on to the Sec translocase system (figure 1.2). Insertion can then proceed through pathways specific for different integral membrane proteins. The Sec pathway involves expenditure of ATP, the energy currency of the cell, to facilitate folding of transmembrane segments as the polypeptide emerges from the ribosome and into the bilayer (Mori and Ito, 2001). Sec-independent pathways also exist and may involve YidC, yet another integral membrane protein (Samuelson *et al.*, 2000). Spontaneous insertion into the membrane has been hypothesized and has been observed for small alpha helical peptides (Popot *et al.*, 1987).

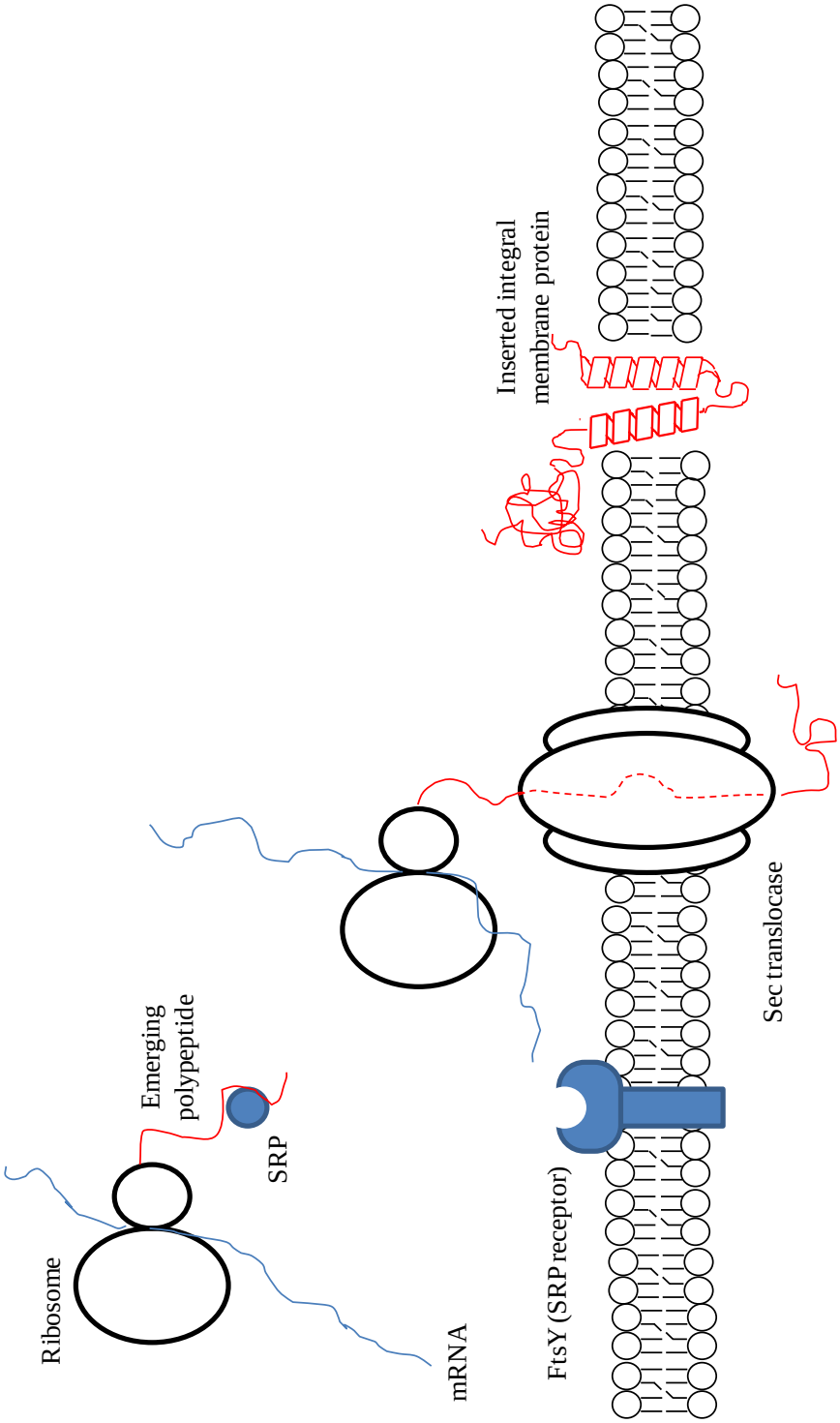

Figure 1.2: Integral membrane protein insertion through the sec translocase pathway.

1.3 Membrane protein expression technologies

Many biochemical tools gather protein data directly from purified protein. Under most circumstances, the protein of interest's natural abundance is not high enough for research purposes. A variety of methods exist to enrich proteins for purification. Cells synthesize proteins through a general pathway beginning from the activation of gene expression to the translation of mRNA into a polypeptide chain. Folding of the polypeptide to form functional protein can then occur. Conveniently, cellular molecular biology can be exploited to synthesize proteins for research or industrial purposes. Selection of host cell types is complex and is largely influenced by the specific protein of interest and how it will be assayed. A common host system is the bacteria, *Escherichia coli* due to widely available and defined expression systems (Choi and Lee, 2004). Fast growth rates of *E. coli* and formation of high density cell cultures are also a boon. However, there are certain drawbacks of using bacterial systems. Foreign membrane proteins can face stability issues in bacteria (Tate, 2001; Tate *et al.*, 2003). The lack of post-translational modifications, incompatible lipid composition, or codon incompatibility of tRNA during the translation step can prevent proper accumulation of membrane protein. Soluble proteins tend to form inclusion bodies when overaccumulated in *E. coli*. Productively, these inclusion bodies of soluble proteins can be easily isolated through differential centrifugation of cell lysate and refolded by a cycle of denaturation and re-naturation (Rudolph and Lilie, 1996; Tsumoto *et al.*, 2003). In contrast, integral membrane proteins must accumulate in the membrane bilayer to remain stable. The bilayer environment protects transmembrane domains from proteolysis. As membrane

protein folding is a co-translational process, refolding inclusion bodies would be time-consuming and tedious. Thus, strategies usually revolve around isolation of membranes containing the protein and selectively reconstituting the protein of interest. Different bacterial strains have as been developed to handle the accumulation of membrane proteins that can have cytotoxic effects (Miroux and Walker, 1996).

Choice of host organism is only the first step in constructing a protein expression strategy. Genetic material encoding the protein of interest must also be introduced to the host system. In bacteria, plasmids are non-chromosomal genetic elements that contain beneficial resistance or metabolic genes. Plasmids can be artificially modified to not only house a particular gene of interest, but also to contain regulatory segments of gene expression. Over-expression and accumulation of membrane proteins can put substantial strain on the host organism (Wagner *et al.*, 2006). Therefore, tunable regulation is necessary for controlling amount of protein produced. The first characterized gene expression regulation system was the *lac* operon in 1961 by Jacques and Monod. Since then, parts of the *lac* operon, particularly the promoter region and the repressor have been engineered into plasmids or host chromosomes to control gene expression. A constitutively expressed *lacI* gene encodes a protein that prevents RNA polymerase from accessing the promoter region preceding the gene preventing gene expression. The *lac* repressor protein can be removed from this promoter region by binding β-galactosides such as the molecule, isopropyl-β-D-1-thiogalactopyranoside (IPTG). In some cases, the *lac*UV5 promoter may not be sufficient to fully repress expression. This is problematic if gene expression prevents cultures from reaching the exponential growth phase. Bacterial

growth beginning from an inoculation into fresh growth media are divided into several phases. The exponential growth phase occurs when cells are rapidly dividing and this is considered the best time to artificially induce gene expression. A lag phase precedes exponential growth and during this phase, bacteria have been observed to be under high oxidative stress as the cell adapts to the new environment and prepares for cell division (Rolfe *et al.*, 2012). Thus, sensitivity to the accumulation of a membrane protein can be heightened at this stage. The *tac* promoter is a derivative of the *lac*UV5 promoter and possesses a tighter interaction with the *lac* repressor protein (Boer *et al*., 1982). Another strategy aims to control expression by using a foreign virus promoter, the T7 promoter that requires a T7 RNA polymerase not naturally found in the host bacterium (Tabor and Richardson, 1985). A coupling of these two expression systems was used and will be described later in this thesis.

1.4 Affinity polyhistidine tagged-membrane protein fusions

Key functional features are often identified through the comparison of wild-type and mutant proteins. The addition or deletion of sequences within a protein can have a significant impact on its structure and function. However, fusing specific polypeptide tags or larger polypeptide domains to a protein is often necessary for additional specificity during selective purification. Advantages of this approach for membrane proteins is that it provides a means for efficient isolation while preserving aspects of secondary and tertiary structure. Usually, large fusions such as the glutathione-S-transferase (GST) or maltose binding protein (MBP) to membrane proteins are avoided. Not only can biological activity of the membrane protein be inhibited, but also the fusion

may not fold properly if it is exposed to the non-cytoplasmic side of the bilayer. Smaller affinity tags are more favorable and in general, have a lesser impact on activity. Several affinity tags have been developed for protein purification (Terpe, 2003) though I will mainly focus on the His_6 affinity tag.

Polyhistidine sequences fused to either end of membrane protein sequences have been used for isolation through immobilized metal affinity chromatography. A 6-histidine (His_6) sequence displays high specificity for transition metal ions such Ni^{2+}, Zn^{2+}, Cu^{2+}, and Co^{2+} (Porath *et al*., 1975). The binding of His_6 to these ions is quite high with a dissociation constant in the range of 10^{-13} M (Hochuli *et al*., 1987). Ideally, the tag itself should not interfere with biological activity due to its small size and lack of a significant net charge. However, some cases where normal protein dimerization was promoted by His_6 tags have been observed (Wu and Filutowicz, 1999). Aside from the affinity tag itself, fusion tags also are composed of a linker region. This linker provides a spacer to physically extend the short affinity region so that appropriate display occurs. An extended flexible region may also be necessary if the tag is to be removed by proteolytic cleavage (Terpe, 2003). The combined sequences of the affinity tag and linker region can alter a membrane proteins topology by influencing the positive inside rule (von Heijne, 1989). A proteolytic site can be engineered to remove the linker and affinity tag sequences. However, the yield depends on the protease cleavage efficiency.

1.5 Integral membrane protein reconstitution

In general, isolation of integral membrane proteins has proven more challenging than the soluble counterparts. In addition to pH, ionic strength, and viscosity, to study

IMP *in vitro* requires that the assaying conditions reflect the lipid bilayer environment. A common solution is the use of detergents. An insufficient hydrophobic environment surrounding the transmembrane regions could lead to aggregation in a polar environment leading to a non-native structural arrangement. As an amphiphillic molecule, detergents can stabilize and solubilise membrane proteins by providing an interface between hydrophobic surfaces and an aqueous polar environment. Choice of detergent is largely based on several factors. The critical micelle concentration (CMC) property of a detergent is a good indicator of how a membrane protein will react with a particular detergent (Arora and Tamm, 2001). The amount of detergent molecules in micelles is equal to the CMC subtracted from the total detergent concentration. Generally, solubilising proteins in detergents solutions of at least 2 times the detergent CMC is recommended to ensure the presence of micelles. Higher concentrations, at least 10 times, is recommended for solubilising proteins from native membranes to counter increased CMC due to the presence of lipids. Determination of the CMC can be variable due to the sensitivity to experimental conditions (le Maire *et al.*, 2000).

1.6 Membrane protein assaying conditions

Due to the sensitivity of integral membrane proteins to non-native conditions (le Maire *et al.*, 2000; Lee, 2004; Seddon *et al.*, 2004), the choice of protein purification strategies can greatly affect the outcome of biochemical and biophysical analysis. 3-D structures from crystallizations of membrane proteins can be hindered by crystallization artifacts due to the detergent used for solubilisation (Loll, 2003). Similarly, peptide fusion tags used for membrane protein purification are often cleaved for crystallization

processes. Depending on the delipidation procedure of a purification technique, membrane proteins can be purified with variable amounts of associated lipid (le Maire *et al.*, 2000). Particular lipids, such as cardiolipin, can play a major role in the structure and function of some membrane proteins (Awasthi *et al.*, 1971). Restoration of membrane protein activity *in vitro* can be accomplished by reconstitution of a detergent-solubilised protein into a lipid environment. Ideally, these conditions mimic the native bilayer more closely than detergent micelles can though residual detergents can carry-over. Aside from detergent-protein solutions, studies can be carried out in liposomes or bicelles where lipid composition can be adjusted (Rigaud and Levy, 2003; Seddon *et al.*, 2002). Appreciably, despite how closely *in vitro* mimics native conditions, *in vivo* experiments are often carried out to verify the predictability of a constructed model system.

1.7 Multidrug resistance

In a world of increasingly antibiotic resistant bacteria there is still little known about the small multidrug transporters of various microorganisms. It is important to understand how these transporters function to develop ways of counteracting bacterial antimicrobial resistance. Alongside other proton-dependent multidrug efflux systems under which those such as the major facilitator superfamily (MFS) and resistance/nodulation/cell division (RND) family are classified, the small multidrug resistance family (SMR) is also a secondary transporter that relies on proton motive force for efflux of its cytotoxic substrates (Paulsen *et al.*, 1996). Members of the SMR family, which appear to be the smallest proteins discovered that can confer multidrug resistance, possess around 110 amino acids and having only 4 transmembrane helices.

In terms of its substrates, these membrane proteins confer resistance to a variety of toxic compounds in the form of QCC (quaternary cationic compounds) and antibiotics (Schuldiner *et al*., 1997). The structures of the QCC used in this study are shown in figure 1.3. A representative member of SMR's is EmrE which possesses 40-50% sequence identity to other species such as SMR's from *Mycobacterium tuberculosis* and *Staphylcoccus aureus* (Bay *et al*., 2007). Thus, it is reasonable to study EmrE and compare it to other members of the SMR subclass. The EmrE monomer possesses 4 transmembrane segments and negative dominance experiments strongly support the hypothesis that the active form is a homo-oligomer (Yerushalmi et al., 1996) though the type of multimerization has yet to be determined. As a membrane protein, EmrE has properties different than their soluble counterparts that make them more difficult to purify and characterize. These are setbacks to obtaining EmrE in high amounts and to obtain protein that imitates the functionality found in nature. Thus, additional tools have been developed to help label and to help isolate these proteins more effectively. One of these tools is the addition of a myc-His_6 tag to the C-terminus of EmrE as was done by Muth and Schuldiner (2000). One part of this tag, the myc-epitope, is a peptide that can be the target of anti-myc antibodies which can have applications in visualizing the protein such as on western blots. Additionally, the his_6 tag is composed of 6 histidines that can be used for chelating metals which is useful for applications such as affinity purification or immobilization on a metal adsorbent. However, addition of peptide chains, in this case to EmrE's C-terminus may markedly influence its activity, folding, topology, and multimeric state as a multi-drug transporter. Structure-wise, various studies propose different multimeric states for the functional unit of EmrE. Some such as cysteine

crosslinking studies support the dimer model for myc-His_6-tagged EmrE (Soskine et al, 2002); the trimeric model has been suggested by some including Muth and Schuldiner (2000) through ligand binding studies. Tagless EmrE has been suggested to be a monomer when EmrE was extracted with 3:1 chloroform:methanol (Winstone et al, 2005). 3-D crystals of tagless-EmrE analyzed by X-ray diffraction reveals its structure to be an asymmetric homo-dimer (Chen *et al*, 2007). Though the earlier crystal structure was retracted due to incorrect calculations (Ma and Chang, 2004), the revised data (Chen *et al.*, 2007) still supports an asymmetric homo-dimer model. This corresponds to the 2-D crystal analyzed by electron cryomicroscopy (Ubarretxena-Belandia *et al*, 2003). These are all just a few studies among many where the myc-His_6 tag could influence EmrE's multimeric state.

As for drug efflux, a decrease in transport activity has been observed in a similar small multidrug transporter, Smr (*Staphylococcal* multidrug resistance protein), where addition of the FLAG epitope (11 amino acids in length) to the C-terminus decreased activity by nearly 30% (Grinius and Goldberg, 1994). The myc-His_6 tag is 27 amino acids long which may suggest an even more marked decrease due to its length. Although *E. coli* possessing EmrE-*myc*-His_6 has been reported to grow in the presence of QCC's (Muth and Schuldiner, 2000), the observation has not been specifically quantified to examine the extent of multi-drug transport activity compared to non-myc-His_6-tagged EmrE. The myc-His_6 tag could provide interference by blocking the pore opening or the substrate could interact with the myc-His_6 tag itself to some extent thereby inhibiting transport. As for topology, the myc-His_6 tag and its linker sequences may present challenges by the effect of the positive inside rule (von Heijne et al, 1992) since the

myc-His_6 tag makes EmrE relatively more negative on the cytoplasmic side as compared to the periplasmic side.

1.8 Bacterial small multidrug resistance proteins

Some forms of bacterial multidrug resistance involve IMP transporters. Protein-mediated drug resistance can also function by modification or degradation of the drug. Cellular mechanisms that do not actively involve protein-drug interactions such as the modification of membrane permeability to the drug also exist. The focus of this discussion will be on protein dependent bacterial multidrug resistance, specifically, on integral membrane drug transporters. This resistance strategy relies on the premise that the efflux rate is higher than the influx of drugs into the cell which is realistic when the extracellular drug concentration is low. There are several classes of multidrug resistance transporters. Among them are the small multi-drug resistance (SMR) class of transporters. As the moniker suggests, the sizes of these transporters range from 100 to 150 amino acids in length. All members of this class are found in bacterial systems. To efflux drugs, SMR are coupled to a proton gradient in an anti-port fashion where the drug effluxes and protons are transported into the cell. There are 3 different SMR sub-types which include the paired SMR (PSMR), the small multidrug pumps (SMP), and the suppressor of GroEL (SUG) subclass. One particular SMP, the *E. coli* multi-drug resistance protein E (EmrE), has been extensively researched and the current knowledge base is comprised mostly from studying this protein. EmrE is comprised of 4 transmembrane alpha helixes with small connecting loops and a small N and C terminus that lack significant secondary structure as was adopted as an archetypal SMP

(Schuldiner *et al.*, 2001). SMR were first characterized by several different groups (Paulsen *et al.*, 1996).

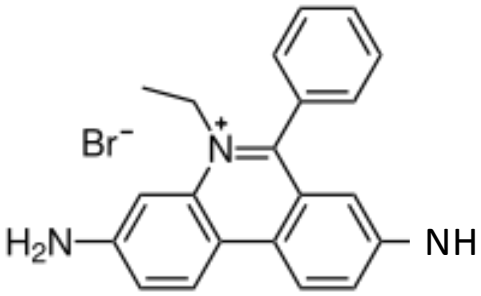

Ethidium (bromide)

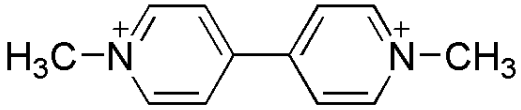

Methyl viologen (dichloride) 2 Cl^-

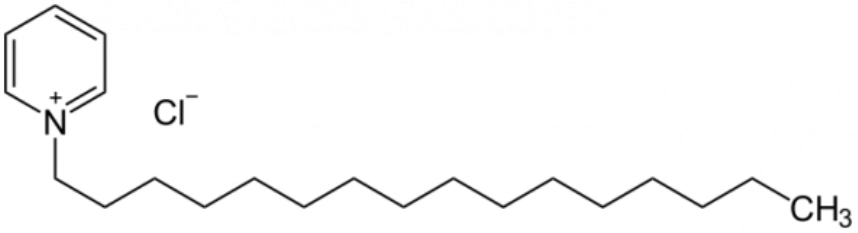

Cetylpyridinium (chloride)

Figure 1.3: Structures of 3 quaternary cationic compounds (QCC). Key structural differences distinguish these molecules: ethidium possesses a flat planar structure; methyl viologen is a divalent cation; and cetylpyridinium has a long alkyl tail.

1.9 EmrE biochemistry

EmrE was first considered an anomaly among membrane proteins when it was discovered that it could possess a dual topology within the plasma membrane (Tate *et al.*, 2003; Ubarretxena-Belandia *et al.*, 2003). This brought a combination of possibilities and difficulties. A dual insertion into the membrane would mean that there was an intriguing insertional mechanism. However, the directionality of transport was not immediately apparent nor the way transport was regulated. Another mystery was the oligomerization of EmrE as it has been observed as a monomer (Winstone *et al.*, 2005), a dimer (Butler *et al.*, 2004), and a tetramer (Ma and Cheng, 2004). Influences of the purification method and assaying conditions may have a large impact on these two structural questions though a direct comparison between the two was never published.

Initially, isolation of EmrE was aided by the use of an organic solvent mixture of 1:1 chloroform:methanol (Yerushalmi *et al.*, 1995). EmrE partitioned into organic solvents rather than into aqueous phases due to its hydrophobicity which was mostly due to short loop regions on the protein. This technique was later optimized for yield by increasing the chloroform:methanol ratio to 3:1 (Winstone *et al.*, 2002). However, the trend shifted from the use of organic solvents to a new strategy employing the use of affinity tags. A 6 histidine (His_6) sequence attached to the C-terminus of EmrE by a peptide linker was engineered (Muth and Schuldiner, 2000). The His_6 had an affinity to divalent metal ions and as such, this new method involved the use of immobilized metal affinity chromatography. Untagged EmrE and tagged EmrE primary structures are compared in figure 1.4. EmrE has been isolated using both of these methods to which current biochemical understanding is attributed. Unfortunately, differences between these

two proteins were not directly compared and it was unclear which was more viable due to conflicting ligand binding values (see table 6.1 in chapter 6). The binding constants of each protein differed by a factor of 2-3 depending on the ligand tested. NMR studies of untagged EmrE in organic solvent have shown that the protein does not remain stable over time whereby the tertiary structure signals were eventually lost (Schwaiger *et al*., 1998). This was puzzling as removal of the organic solvent reconstitution of the EmrE into proteoliposomes resulted in functional transport (Yerushalmi *et al*., 1995). Furthermore, tertiary structure of EmrE was not been determined until recently with the reconstitution of EmrE into bicelles (Morrison *et al.*, 2012) and this was only with an affinity tagged EmrE. For the purposes of this study, untagged EmrE will refer to the EmrE isolated using organic solvents and the tagged EmrE will refer to the construct isolated using affinity purification.

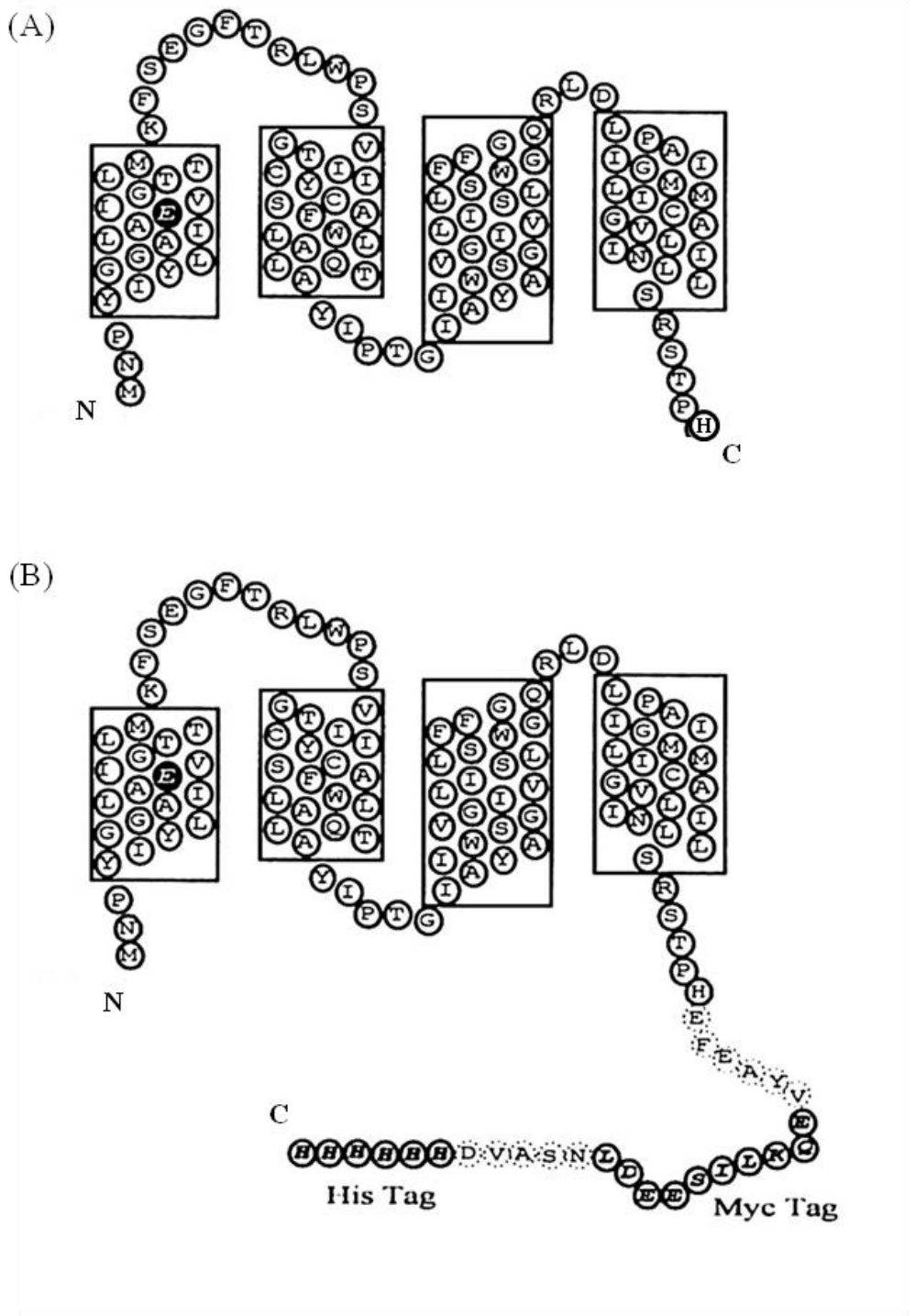

Figure 1.4: Diagram of (A) Untagged and (B) Tagged EmrE amino acid sequences for comparison. Figures were modified from the original found in Muth and Schuldiner (2000) where boxes indicated transmembrane regions predicted by hydropathy plots.

1.10 Goals and aims

The goal of this study was to compare the effects of the purification method on the structure and function of EmrE. Specifically for this comparison, the purification methods used were developed to be as identical as possible to the His_6 affinity purification (Muth and Schuldiner, 2000) and the organic solvent purification (Winstone *et al.*, 2002). The following aims were accomplished to reach this goal:

- Untagged EmrE was isolated from batch culture and reconstituted into a buffer containing the detergent, DDM.
- Site-directed mutagenesis was performed to obtain the appropriate tagged EmrE gene.
- Tagged EmrE accumulation in culture was optimized.
- A series of chromatography steps were used to isolate tagged EmrE from bacterial membranes.
- Fluorescence spectroscopy was used to examine differences in untagged vs. tagged EmrE conformation.
- Fluorescence emission spectra were collected using different excitation wavelengths to probe solvent dynamics within untagged and tagged EmrE.
- Ligand binding with 3 different EmrE substrates was monitored by fluorescence to compare binding affinities.
- A resistance assay was performed to assess transporter activity *in vivo.*

Chapter Two:

Chapter Three: **Materials and methods**

3.1 Strains, plasmids, and molecular biology

The primary goal was to compare untagged EmrE and tagged EmrE. Both proteins had been previously isolated in a specific manner and thus, the aim was to obtain these proteins using the respective methods reported by Winstone *et al* (2002) for untagged EmrE and Miller *et al* (2009) for tagged EmrE. A *recA1* deficient strain, DH5α, was used for the molecular biology work to avoid DNA recombination issues, especially with the gene of interest.

3.1.1 Untagged emrE

For protein purification, untagged EmrE was expressed in *E. coli* strain LE392Δunc (*F¯, supE44, supF58, hsdR514, galK2, galT22, metB1, trpR55, lacY1, ΔuncIC*) (Turner *et al.*, 1997). An important feature of this strain was the *unc* gene deletion which encodes the c-subunit of the *E. coli* F_1F_0-ATPase. Downstream procedures involved an extraction step using organic solvents where EmrE and the ATPase subunit can undesirably co-partition into the organic solvent fraction (Ksenzenko and Brusilow, 1993).

The plasmid pEmr11 was transformed into the LE392Δunc strain. This plasmid was derived from pMS119EH (Furste *et al.*, 1986) and encodes *emrE* in the multiple cloning site as previously described by Winstone *et al.* (2002) (see figure 2.1 for plasmid map). The *lac* repressor gene is also encoded in the plasmid and expression was

controlled by the inducible *tac* promoter, a *trp* and *lac* promoter hybrid (Boer *et al*, 1983).

3.1.2 Tagged emrE

Tagged *emrE* was expressed in the *E. coli* strain C43(DE3) (*F*⁻ ompT hsdSB (rB-mB-) gal dcm (DE3)) (Miroux and Walker, 1996) and encoded by the plasmid pTZEmrEmH6 (plasmid pTZ-19R encoding *emrE-myc-His*$_6$, see figure 2.1 for plasmid map).

3.2 Mutagenesis to generate tagged emrE

To start, the plasmid pEmrE-*myc-His*$_6$ was available from previous molecular biology work by Denice Bay. Briefly, pEmrE-*myc-His*$_6$ was constructed by "cross-stitch" PCR using 3 different primers on pEmr11, the original plasmid template. A *myc-His*$_6$ sequence was appended to the untagged *emrE* gene sequence such that when expressed, the peptide tag would be on the C-terminal end of the EmrE. However, there was a modification of sequence in the linker region between the *emrE* gene and the *myc-His*$_6$ to create a XhoI restriction site for the intention of removing the tag. As the eventual aim was to compare a tagged EmrE isolated in a similar manner to what was reported in Miller *et al* (2009), it was necessary to change the sequence. The amino acid sequence of this 28 amino acid fusion tag encoded by pEmrE-*myc-His*$_6$, beginning from the residues following His110 of the EmrE protein corresponds to NH_2- <u>L</u>EFEAY [V] EQK LISEEDLNSAVDHHHHHH- CO_2H. This change required the removal of a codon encoding a leucine (underlined) and the addition of a codon encoding a valine (in square brackets). Two sets of primers for two individual site-directed mutagenesis procedures

were designed for this purpose. The first set of primers was designed for a leucine codon deletion. 19-21 base pairs flanked the site of deletion for annealing purposes (figure 2.2). Similarly, the second set of primers for the valine insertion had 18-19 base pairs flanking the site desired for the valine codon insertion (figure 2.2). The desired sequence was confirmed by DNA sequencing using a high-throughput 96-capillary Applied Biosystems 3730xl sequencer.

(A)

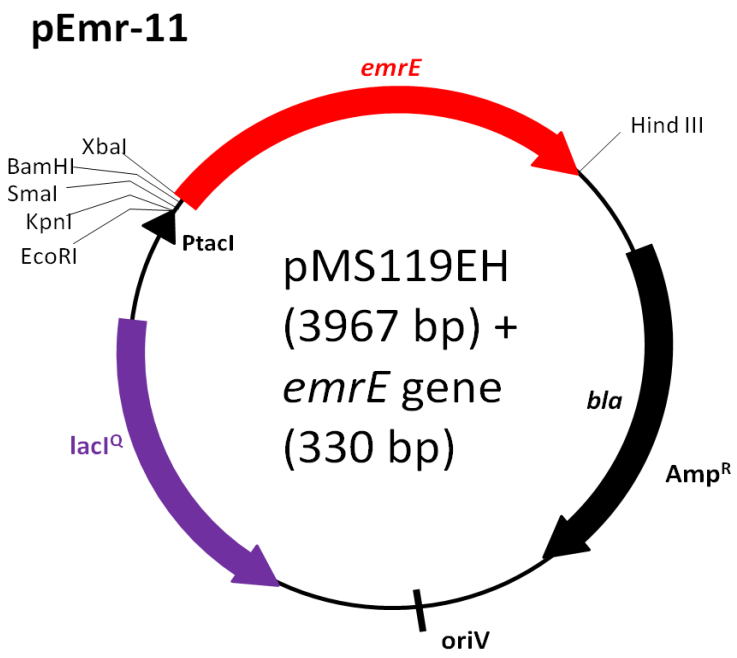

(B)

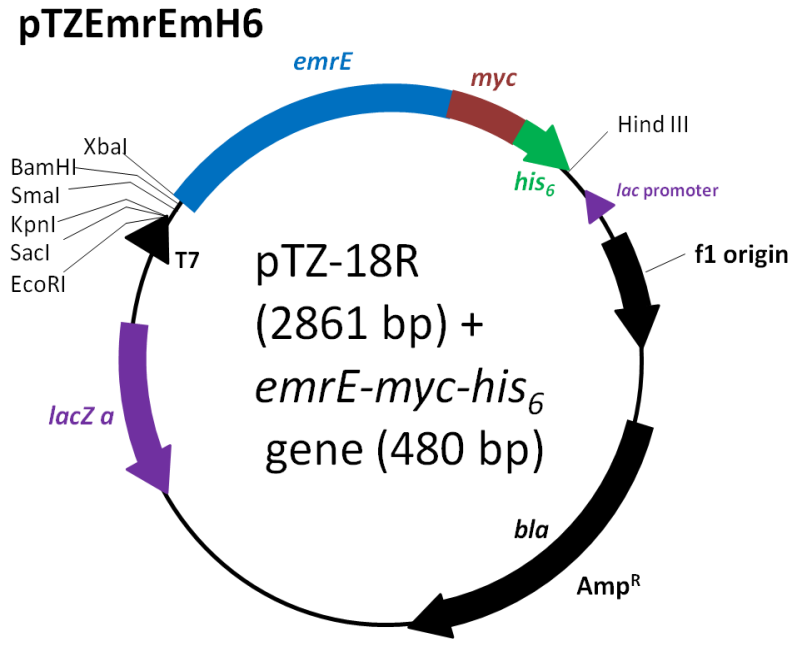

Figure 2.1: Plasmid maps of (A) pEmr11 and (B) pTZEmrEmH6 encoding untagged and tagged EmrE, respectively.

The plasmid was named pEmrEmLVH6 which had the correct mutagenesis product between the XbaI and HindIII restriction sites of the vector pMS119EH. This plasmid was used for the resistance assays described in section 2.10. pEmrEmLVH6 contained the correct mutagenesis product, however expression was under the control of a *tac* promoter whereas a T7 promoter was reported (Miller *et al*, 2009). Thus, further manipulations were necessary to sub-clone the gene into a suitable plasmid with a T7 promoter. For expression utilizing a T7 promoter, the destination plasmid, pTZ-18R was selected. The tagged *emrE* gene was sub-cloned into the plasmids pTZ-18R and pTZ-19R using the restriction enzymes XbaI and HindIII and the T4 DNA ligase. The resulting plasmid of the pTZ-18R and tagged *emrE* ligation was named "pTZEmrEmH6" and was used for tagged EmrE purification (see figure 2.1). The other plasmid, pTZ-19R is identical to pTZ-18R save for the multiple cloning site which has the same restriction sites as pTZ-18R although in a reversed order with respect to the T7 promoter. This was useful as a control for later assays and the plasmid was named "pTZ6HmErmE". Expression in the DH5α strain was not possible due to an absence of the gene encoding the T7 polymerase on the pTZ-18 and 19R plasmids. As a T7 polymerase is necessary for gene transcription, the plasmid was transformed into C43(DE3), an *E. coli* strain containing a chromosomal T7 polymerase under the control of a lacUV5 promoter (Miroux and Walker, 1996).

LDEL forward primer sequence:

5' - G TCA CGA AGC ACA CCA CAT (*) GAG TTC GAG GCT TAT GAG CAG – 3'
LDEL reverse primer sequence:

5' – CTG CTC ATA AGC CTC GAA CTC (*) ATG TGG TGT GCT TCG TG A C – 3'
VINS forward primer sequence:

5' – A CAT GAG TTC GAG GCT TAT GTC GAG CAG AAG TTA ATT AGC – 3'
VINS reverse primer sequence:

5' – GCT AAT TAA CTT CTG CTC GAC ATA AGC CTC GAA CTC ATG T – 3'

Figure 2.2: Primer pairs used for site-directed mutagenesis resulting in a deletion of a leucine codon (LDEL primer set) and insertion of a valine codon (VINS primer set) in the linker region of tagged EmrE. The (*) marks the position of the leucine codon on the template DNA. The underlined GTC codon marks the position of insertion of a valine codon on the template DNA.

3.3 Dot blot analysis of tagged EmrE protein accumulation in *E. coli* culture

Cultures of C43(DE3) containing either pTZEmrEmH6, pEmrE-*myc*-*his*$_6$, or pTZ6HmErmE were grown overnight in 3 mL of LB containing 0.1 mg/mL ampicillin in a 37°C shaking incubator . The next morning, 500 µL of overnight culture was added to a 250 mL capped flask containing 50 mL of LB and 0.1 mg/mL ampicillin. Each flask culture was induced with 0.1, 0.3, or 0.5 mM IPTG when the OD_{600} reached 0.5. 2 µL aliquots were spotted onto a nitrocellulose membrane directly from each culture before IPTG was added at OD_{600}, and at 1, 2, and 3 hours after IPTG addition. 2 µL of a 3 µg/mL and 0.3 µg/mL solution of tatA-*myc*-*His*$_6$, a component of the bacterial twin arginine translocase, was also spotted onto the nitrocellulose membrane as a positive control against the INDIA HisProbe-HRP antibody (Thermo-Scientific). This antibody is specific to 6- histidine sequences and is conjugated with horseradish peroxidise (HRP). Once the spots were air-dry, the nitrocellulose membrane was blocked in 40 mL of tris-buffered-saline (TBS; 50 mM Tris-HCl, pH 7.5, 200 mM NaCl) containing 2 g of skim milk powder for 1 hour at room temperature. The membrane was washed twice with 3.5 mL of TBST (TBS containing 0.05% v/v Tween20) for 5 min each. Afterwards, the membrane was placed in a solution containing 5 µg/mL of the INDIA HisProbe-HRP for 1 hour. After incubation of the membrane with the antibody, the blot is placed in a solution containing 4-chloro-1-naphthol and hydrogen peroxide (Bio-Rad HRP Conjugate Substrate Kit) for 10-30 minutes. HRP catalyzes an oxidation reaction between hydrogen peroxide and 4-chloro-1-naphthol to form the colored precipitate, 4-chloro-1-naphton. Colored spots developed on the nitrocellulose membrane where antibody bound the His_6-tag.

3.4 Growth curves of *E. coli* accumulating tagged EmrE

Freshly transformed cultures of C43(DE3) with either the plasmid pTZEmrEmH6 or pTZ18R (empty vector) were incubated overnight in test tubes containing 6 mL of lysogeny broth (LB) and 0.1 mg/mL ampicillin in a 37°C shaking incubator. 200 µL of the culture was used to inoculate a 20 mL culture of LB and 0.1 mg/mL ampicillin in a 250 mL Erlenmeyer flask (a 1/100 dilution). The optical density at 600 nm (OD_{600}) was recorded for the overnight culture and divided by 100 to get the OD_{600} at time zero (t = 0). The OD_{600} of the 20 mL culture was recorded every hour for 8 hours after time zero. Cultures were induced when the cultures reached the mid-log phase of growth (between OD_{600} = 0.4-0.6) with 0.3 mM IPTG.

3.5 EmrE purification procedures

3.5.1 Lysogeny broth

The lysogeny broth (LB) solutions used throughout this study were made with 50% less NaCl than the standard LB. Unless otherwise noted, all LB in this study refers to this "half-salt" LB (5 g/L yeast extract, 10 g/L tryptone, and 5 g/L of NaCl). The reduction of NaCl in the growth media enabled cultures to reach stationary phase in a shorter time period (data not shown).

3.5.2 Accumulation of untagged EmrE in batch culture

LE392Δ*unc* cells containing the pEmr11 plasmid were cultured in 1 L batches of terrific broth (TB) (12 g/L tryptone, 24 g/L yeast extract, 0.4% v/v glycerol). Each 1 L batch was inoculated with 10 mL of overnight culture in Lysogeny broth (LB) (10 g/L

tryptone, 5 g/L yeast extract, 5 g/L NaCl) that was in turn inoculated from frozen cell stock (saturated cells in 8% dimethyl sulfoxide in LB). All cultures contained 0.1 mg/mL ampicillin to maintain the plasmids during cell growth. The cultures were incubated at 37°C and growth was monitored using optical density measurements at 600 nm (OD_{600}). Once the OD_{600} of the cultures reached 0.5-0.7 (approximately 3 hours), isopropyl β-D-1-thiogalactopyranoside (IPTG) was added to a final concentration of 0.1 mM per 1 L batch of culture. Cultures were further incubated at 37°C in a shaking incubator for another 3 hours before harvesting by centrifugation at 5,000 x g for 10 minutes at 4°C. Cell were washed by suspending the pellet in SMR A buffer (50 mM MOPS, pH 7.5, 5 mM EDTA, 1 mM DTT, 8% w/v glycerol) by stirring. The cells were re-pelleted by centrifugation at 4,000 x g for 10 minutes at 4°C. The supernatant was discarded and the weight cell weight was recorded (around 4 g per 1 L batch of culture). The pellet was resuspended in 1-2 mL of SMR A buffer per gram of the wet cell weight. Phenylmethylsulfonyl fluoride (PMSF), a serine protease inhibitor, was added to the cell slurry to a final concentration of 0.1 mM before storing at -80°C.

Frozen cell suspensions were thawed and poured into a 4°C pre-chilled 40 mL capacity Sim Aminco French Pressure cell. The suspensions were passed through the French Press twice at around 10,000 psi to lyse the cells. Unbroken cells were separated by centrifugation at 2,000 x g for 10 min to yield the low-speed pellet (LSP). The supernatant was further centrifuged at 120,000 x g for 90 min at 4°C to collect the membrane pellet. The cytosolic fraction (supernatant) was removed and the membrane pellet resuspended by hand held homogenization in SMR A buffer. This membrane

fraction was stored at -80°C and only thawed once the necessary preparations for the extraction step were made (see below).

Protein concentrations of a small 100 µL aliquot of the membrane solution were determined by using a modified Lowry Assay (Markwell et al, 1978). SDS was present in this assay to assist in solubilising membrane proteins. Bovine Serum Albumin (BSA) was used as a protein standard as it was relatively inexpensive in high quantities and in high purity. The protein concentration of each suspension was determined using a linear BSA standard curve where linearity was maintained between 1 µg and 50 µg.

3.5.3 Chloroform: methanol extraction and size-exclusion chromatography

A frozen membrane resuspension was thawed and diluted with SMR A buffer (50 mM MOPS, pH 7.5, 5 mM EDTA, 1 mM DTT, 8% w/v glycerol) to a total protein concentration of 10 mg/mL. 10 mL of this sample was then poured into a 500 mL separatory funnel containing 300 mL of 3:1 $CHCl_3$:CH_3OH. 50 mL of double distilled water (ddH_2O) was added to the funnel to separate the organic and aqueous phases. The contents of the funnel were mixed by inverting periodically 3 times at 15 minute intervals. The phases were then allowed to separate for at least 3 hours in a fumehood with the hood-light off to minimize tryptophans from reacting with the chloroform as observed by Ladner et al (2004). The lower organic phase was drained into a clean beaker, divided into 6 x 50 mL falcon tubes and centrifuged for 10 minutes at 2,000 x g at room temperature. Tubes were carefully removed from the rotor as to prevent perturbing of the surface carry-over aqueous phase. Approximately 5 mL off the surface of each tube was siphoned off to ensure negligible carry-over. The remaining contents were

pooled into a 500mL – 1 L round-bottom flask. A rotovap was used to reduce the volume to 2 mL or until precipitation began to form. The remaining volume was transferred to a glass test tube, stoppered, and covered in aluminum foil. The sample was loaded into a SR-25 column (GE Healthcare) containing sephadex LH-20 resin for size exclusion chromatography to further separate the protein from lipids. An AKTA purifier was used to facilitate sample loading and elution using 1:1 $CHCl_3$:CH_3OH. 3 peaks were observed and aliquots from each were collected (figure 2.3). A downstream SDS-Tricine PAGE analysis of the samples showed peaks corresponding to the untagged EmrE monomer and homo-oligomer molecular weights in the first eluted fraction (figure 3.3). Fractions were placed under a stream of N_2 gas until a dry grainy white powder remained. The samples were stored at -20°C. These samples were solubilised in a DDM containing buffer (DDM buffer: 20 mM Tris-HCl, pH 7.5, 150 mM NaCl, 0.08% *w/v* DDM) before assaying.

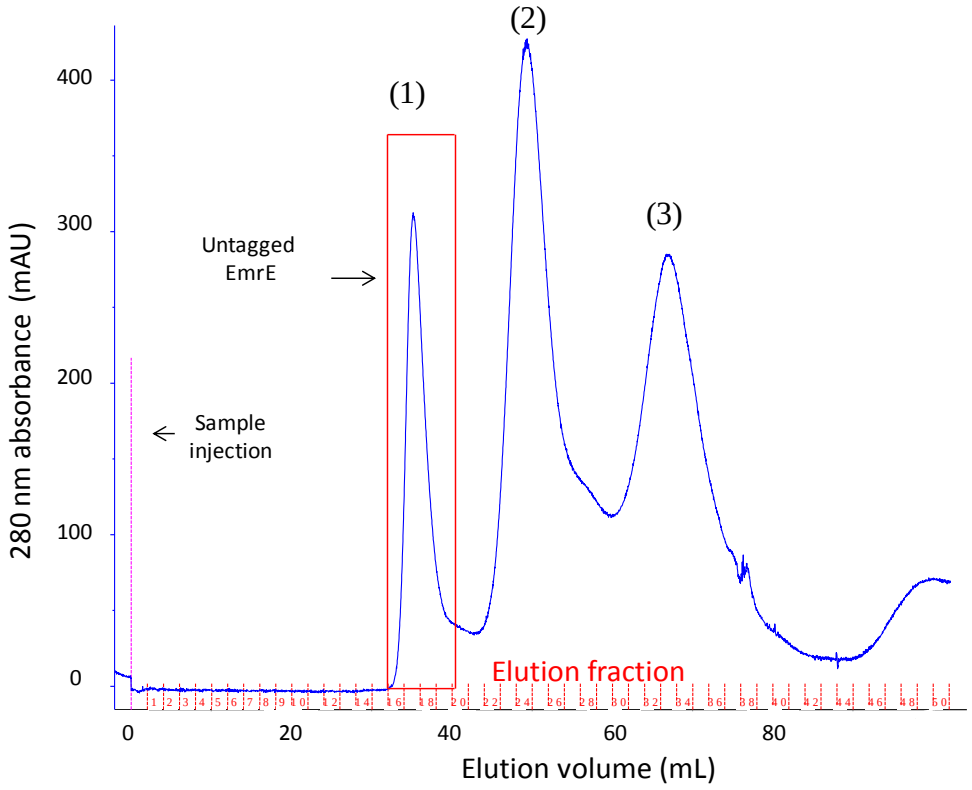

Figure 2.3: Elution profile of untagged EmrE through a SR-25 column (GE Healthcare) filled with sephadex LH-20 resin. Sample was eluted with 1:1 chloroform:methanol monitored at 280 nm using an AKTA purifier (GE Healthcare). The first peak fraction contained untagged EmrE as confirmed on a downstream SDS-Tricine PAGE. On the other hand, the presence of EmrE was not confirmed in the second and third peak fractions. Further analysis on these peaks were not deemed necessary and were not carried out for the purpose of this study.

3.5.4 Accumulation of tagged EmrE in batch culture

C43(DE3) cells containing the pTZEmrEmH6 plasmid were cultured in 1 L batches of LB broth instead of the Terrific broth (TB) that was used for untagged EmrE cultures. Otherwise, growth conditions were the same as for untagged EmrE expression and purification until induction of cultures with IPTG (see previous). When cultures reached an OD_{600} of 0.5 - 0.7 (approximately 4 - 4.5 hours), cultures were induced with 0.3 mM IPTG. Cells were harvested in a similar manner as described previously for untagged EmrE cultures except that cell resuspension buffer (20 mM Tris-HCl, pH 8.2, 50 mM NaCl) was used in place of SMR A buffer. Cell suspensions were stored at -80°C.

Frozen cells were thawed and lysed using a French Pressure cell (as described for the untagged EmrE preparation). The membrane pellet obtained from 6 L of batch culture was resuspended in 25 mL of a membrane solubilisation buffer (40 mM Tris-HCl, pH 8.2, 100 mM NaCl, 4% w/v DDM, 10 mM 2-mercaptoethanol) using hand-held homogenization. The resuspension was placed in 50 mL falcon tubes on a gently rocking incubator at 4°C overnight to be prepared for Nickel-affinity chromatography the next morning.

3.5.5 Immobilized nickel affinity chromatography

The bacterial membrane resuspensions from the previous day were diluted 1:1 with ddH_2O and centrifuged at 60,000 x g to pellet non-solubilized material. NaCl and imidazole was added to the resuspension to final concentrations of 350 mM and 15 mM, respectively.

Using an AKTA purifier (GE Healthcare), the sample was loaded into a 5 mL HisTrap FF column (also from GE healthcare) which is an immobilized nickel column with affinity to polyhistidine sequences. The column was then washed with 20 column volumes (CV) of Wash Buffer 1 (20 mM Tris-HCl, pH 8.3, 400 mM NaCl, 15 mM imidazole, 0.1% w/v DDM, 5 mM 2-mercaptoethanol), 20 CV of Wash Buffer 2 (20 mM Tris-HCl, pH 8.3, 20 mM NaCl, 15 mM imidazole, 0.1% w/v DDM, 5 mM 2-mercaptoethanol), and 10 CV of Elution buffer (20 mM Tris-HCl, pH 8.3, 25 mM NaCl, 200 mM imidazole, 0.1 % w/v DDM, 5 mM 2-mercaptoethanol). A single elution peak was observed above the baseline and the corresponding elution fractions were collected (figure 2.4A).

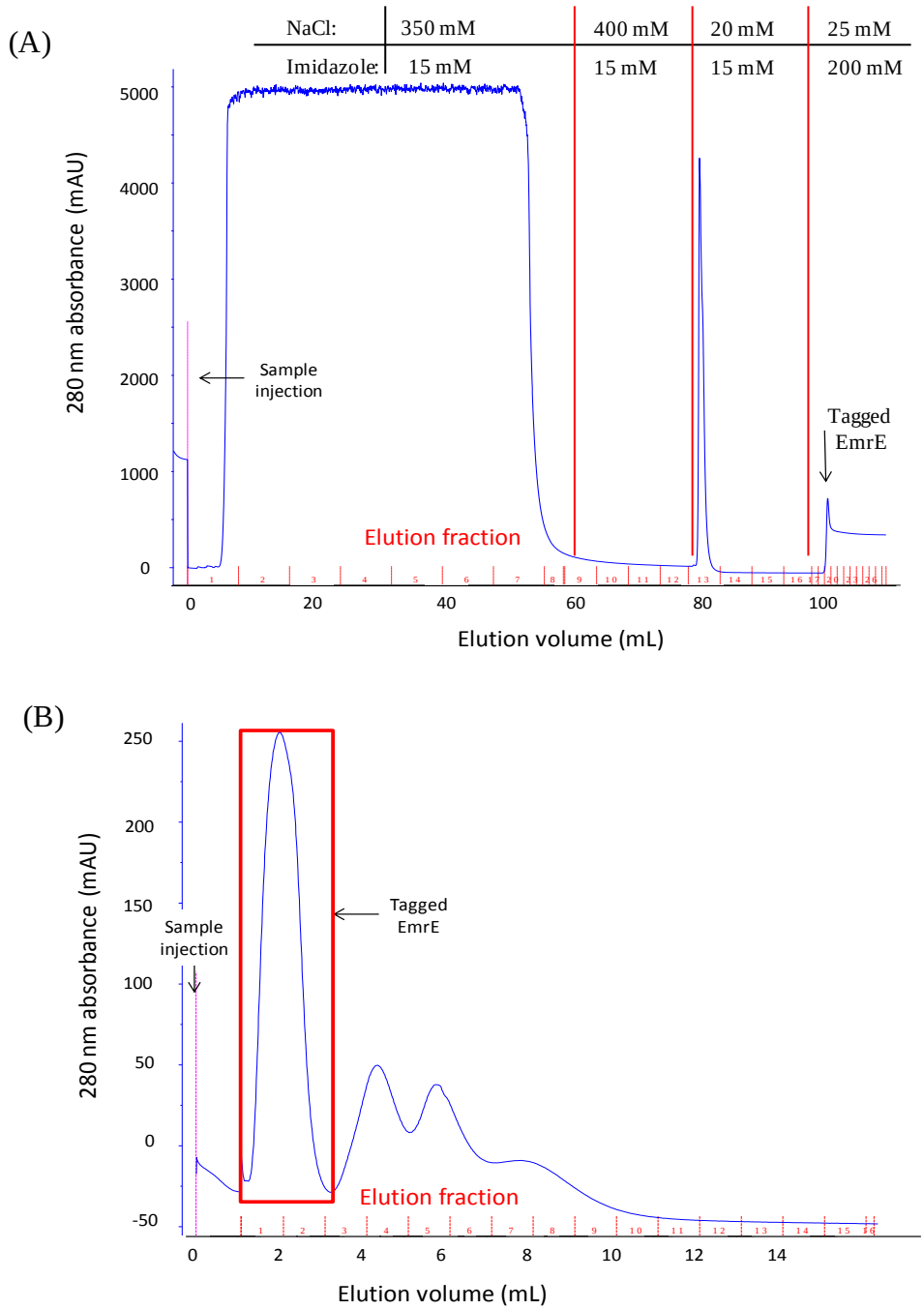

Figure 2.4: Tagged EmrE elution profiles from (A) an immobilized nickel affinity chromatography using a 1 mL HisTrap FF column (GE Healthcare). (B) a 5 mL HiTrap desalting column.

3.5.6 HiTrap desalting chromatography

Eluted fractions from the HisTrap column were loaded into a 5 mL HiTrap desalting column (GE healthcare) in 2 mL injections to remove the imidazole as it can cause spectral interference. The column was equilibrated with DDM buffer (20 mM Tris-HCl, pH 7.5, 150 mM NaCl, 0.08 % w/v DDM) and the sample was exchanged into this buffer. The first peak was collected which was expected to be the protein as larger molecules elute away from smaller buffer components in a size exclusion column (figure 2.4B). A 10 µL aliquot of the HiTrap desalting eluted fraction was analyzed on an SDS-Tricine PAGE to confirm the presence of a ~14 kDa band corresponding to the molecular weight of monomeric tagged EmrE. Subsequent analysis by western blotting techniques using the INDIA- HisProbe-HRP anti-His_6 antibody identified the band as His_6-tagged protein. A similar band was not observed in the flow-through and the 2nd wash peak fraction on the SDS-Tricine PAGE. Tagged EmrE samples in DDM buffer were stored at $-20^{o}C$.

3.6 SDS-Tricine PAGE analysis

10 µL of tagged EmrE in DDM buffer (from the HiTrap desalting elution) was incubated with 5 µL of Laemmli solubilisation buffer (LSB: 12% w/v SDS, 30% v/v glycerol, 0.05% w/v Coomassie brilliant blue G250, 150 mM Tris-HCl, pH 7.0, 100 mM DTT) for 1 hour before loading into the PAGE gel. Similarly, a 200 µL aliquot of the 6 mL size exclusion chromatography elution that was solvent-evaporated was solubilised by adding 10 µL of ddH_2O and 5 µL of LSB and incubated for 1 hour before loading into the PAGE gel. Note that the relative concentrations did not matter and were not measured

beforehand as this gel was performed with the sole aim of determining the success of each purification method in isolating the intended protein. Upon running the electrophoresis to completion, the gels were incubated in a 50% methanol, 0.1% v/v Trichloroethanol (TCE) solution for approximately 15 minutes. TCE reacts with tryptophans found in both untagged and tagged EmrE under UV-light. Bands on the gel were visualized under UV-irradiation at 300 nm (as described by Ladner et al, 2004).

3.7 Fluorescence

Fluorescence spectra of each EmrE sample were collected using a Fluorolog-Tau-3 Time-resolved spectrofluorimeter. This spectrometer was ideal for membrane protein samples as it had a dual monochromator on the excitation side which helps decrease the light scattering from particulates. Emission is collected with a single grating monochromator. The instrument is at the cutting edge with excellent signal to noise for dilute samples. Sample spectra were collected in 1 cm quartz cuvettes using a 295 nm excitation wavelength to specifically select for tryptophan fluorescence. The emission spectra were collected between 300 nm and 400 nm to avoid the collection of scattered light. A 5 nm slit width was used for both excitation and emission windows and data was collected through the S/R channel. The interval was set at 0.5 nm and integration time at 0.1 s. Each spectrum collected was an average of 3 scans.

3.8 Red edge excitation shift spectra collection

Sample spectra were collected in a 1 cm quartz cuvette. Emission spectra were collected between 300 nm and 400 nm with an integration time of 0.2 s and in intervals of

2 nm. The slit width was set at 5 nm for both excitation and emission. Collected emission spectra represented an average of 6 scans. The series of excitation wavelengths used were set at 260, 265, 270, 275, 280, 285, 290, 295, 300, and 305 nm. Emission spectra corresponding to each excitation used were collected individually. Emission spectra of DDM buffer that did not contain the EmrE protein were also collected in this way. This was subtracted from the corresponding EmrE emission spectra so that only signals from the EmrE were monitored. The λ_{max} of each EmrE spectra was determined and plotted against the excitation wavelength to obtain a REES plot (Red-edge excitation shift).

3.9 Ligand binding

Initially, a range-finding assay was performed using ethidium concentrations from a previous ligand binding study (Winstone et al, 2002) as a guideline. 10 nM of either untagged or tagged EmrE in DDM buffer was titrated with a solution of 1 mg/mL ethidium bromide in water (see table 2.1 for titration scheme). Fluorescence spectra using a 295 nm excitation were collected after each volume of ligand added. A small magnetic stir bar was added to the 1 cm path-length quartz cuvette containing either the sample or buffer. The stirring speed was set such that the surface was not noticeably disturbed. Approximately 1 minute was allowed between the addition of ligand and the beginning of spectra collection. The cuvette and stir bar were rinsed with water 6 times followed by ethanol twice and then dried under a vacuum before assaying a new solution. Further range-finding was not required as saturation was reached within the range tested with ethidium (table 2.1). A total of 3 replicates were performed with the first sample preparation to control for experimental variability. After this, only 1 experimental

replicate of the following 2nd and 3rd sample preparations were performed. Thus, each ligand binding curve reflects the average of 3 replicates from 3 different protein preparations to control for biological and preparation variability.

3.9.1 Fluorimeter parameters during ligand titration

Unlike the collection of fluorescence spectra described in section 2.7, a 10 nm slit width was used for both excitation and emission. The interval was set at 2.0 nm and the integration time at 0.1 s. Only 1 scan of the emission between 300 and 400 nm was collected per titration. 295 nm excitation was used to select for the tryptophans in the EmrE samples. Samples were diluted and assayed in a 1 cm quartz cuvette at room temperature.

3.9.2 Ligand and baseline signal considerations

A blank titration of DDM buffer alone without EmrE was performed to observe the baseline signal. All ligands were titrated to near saturation based on a ligand concentration where further titrations resulted in little to no observable change in the fluorescence intensity.

3.9.3 Range-finding assays

Range finding assays were carried out for each ligand used in this study. The ethidium titrations reached near saturation levels at the end of titration set #1 in table 2.1. However, a second titration set (#2, see table 2.1) was required to reach saturation for the other two ligands, MV and CTPC. Further titrations using the 1 mg/mL QCC solution

was not performed as dilution effects became prohibitive. Thus, the 2nd titration set was with a solution of 10 mg/ mL QCC. Saturation was achieved only for MV using this new titration set. Range-finding was not pursued further for CTPC as binding curve extrapolations to concentrations as high as 2500 times the amount of EmrE would only reach 70% saturation of binding sites. Both QCC were also titrated into a blank solution that did not contain any EmrE protein and the fluorescence emission spectrum was recorded. The blank solution's emission spectrum was subtracted from sample spectrum at corresponding titrant concentrations. This was to take into account the changes in intensity due to ligand concentration effects (e.g. – self-quenching).

3.9.4 Dilution effects and lamp intensity

Another factor influencing fluorescence intensity was dilution effects resulting from increasing volume as the ethidium solution was added. Initially, the sample cuvette contained 2 mL of sample or buffer and resulted in a final volume of approximately 2.2 mL. A 1.6 µM solution of *n*-acetyl-tryptophan amide (NAWA) was titrated with water in place of the ethidium bromide solution following the titration scheme in table 2.1. The intensity change between each titration would solely be due to dilution effects. This individual percent change between each titration step was then subtracted from the total contributions of the ethidium bromide titrations at the time of analysis. The 1.6 µM concentration was initially chosen to reflect the amount of tryptophans in a 0.4 µM EmrE solution. Though this EmrE concentration was never assayed, it was recognized that percent intensity changes due to dilution should remain concentration independent and would still apply to the assayed EmrE concentrations of 10 nM. Percent intensity changes

due to dilution were directly subtracted from EmrE-ligand titrations percent intensity changes at the corresponding titration volume. To conserve sample, sample volume was eventually reduced from 2.0 mL to 1.5 mL for all biological replicates following the first biological replicate. The titration volumes were also reduced accordingly by a factor of 0.75 while using the same ligand stock concentration (1 mg/mL or 10 mg/mL) to keep ligand concentrations consistent.

As multiple titrations were performed in one day, the fluorescence lamp intensity could fluctuate between experiments. To control for this, the spectra of a 1.6 µM NAWA solution was collected before each set of titrations to represent the lamp intensity of that set of titrations. A new 1.6 µM NAWA solution was freshly prepared each time. Each set of titrations were normalized to the fluorescence emission intensity at 360 nm of the 1.6 uM NAWA solution representing the baseline titrations. A change in lamp intensity would be reflected in the NAWA solution emission intensities and these were used to correct for resulting baseline intensity shifts.

Table 2.1: Ligand binding titration order

Titration set #1 (titrations from 1 mg/mL ligand)				Titration set #2 (titrations from 10 mg/mL ligand)			
Titration	Ligand concentration (µg/mL)	Volume of titrant (µL)*	Total volume (µL)*	Titration	Ligand concentration (µg/mL)	Volume of titrant (µL)*	Total volume (µL)*
1st	2	4	2004	14th	68	4	2108
2nd	4	4	2008	15th	87	4	2112
3rd	6	4	2012	16th	106	4	2116
4th	8	4	2016	17th	125	4	2120
5th	10	4	2020	18th	143	4	2124
6th	12	4	2024	19th	162	4	2128
7th	14	4	2028	20th	180	4	2132
8th	18	8	2036	21st	217	8	2140
9th	22	8	2044	22nd	253	8	2148
10th	25	8	2052	23rd	289	8	2156
11th	31	12	2064	24th	343	12	2168
12th	40	20	2084	25th	431	20	2188
13th	49	20	2104	26th	518	20	2208

*note: 3 biological replicates were performed, the 1st used the titration scheme as listed in the table. The 2nd and 3rd titrations used the same titration scheme except that all volumes listed in this table were reduced by a factor of 0.75.

3.10 Resistance assays

For QCC-resistance assays, the *E. coli* K12 strains BW25113 (*lacI*^{q}, *rrnB*$_{T14}$, *ΔlacZ*$_{WJ16}$, *hsdR514*, *ΔaraBAD*$_{AH33}$, *ΔrhaBAD*$_{LD78}$) and JW0451 (the same as the BW25113 genotype with an additional gene deletion of *acrB*) were used. Untagged and tagged EmrE were cloned in the vector pMS119EH resulting in the plasmids pEmr11 (Winstone *et al*., 2002) and pEmrEmLVH6, respectively. Cells were cultured on a LB streak plate containing 0.1 mg/mL ampicillin. Colonies were picked and mixed into a 0.9% saline solution until the turbidity matched a 1.0 Mcfarland standard. The solution was then used to inoculate 96-well plates containing LB growth media and a dilution series of QCC (either ethidium, methyl viologen, or cetylpyridinium). The QCC serial dilution began at a concentration of 5 mg/mL in a well and continued to 9.8 µg/mL in a dilution step of ½ of the concentration of the preceding well. A well that did not contain QCC was also included. Spot plates containing LB + 0.1 mg/mL ampicillin were used to verify the concentrations estimated by the 1.0 Mcfarland standard. Spot plates were incubated for 12-16 hours at 37°C before counting colonies. Growth plates were also incubated at 37°C in a shaking incubator containing a basin of water on a separate rack to prevent evaporation of the media. 96-well plates were removed from the incubator every hour to record the optical densities of each well at 550 nm (OD_{550}) using a plate reader. This was repeated over the course of 11 hours. Plates were further incubated at 37°C until 26 h after inoculation and a final end-point OD_{550} was recorded. A series of "blank" wells containing only growth media or growth media and QCC was included on the plates and the optical density values were subtracted from the sample data sets. Data collected reflected the average of 3 experimental replicates and 3 biological replicates (from

cultures on different streak plates). EmrE expression was uninduced as no IPTG was added to the growth media.

Chapter Four: **Protein purification**

4.1 Optimizing tagged EmrE protein accumulation in batch culture

Only tagged EmrE methods required optimization as a routine protocol had not been previously established. An untested plasmid containing the tagged *emrE* gene was obtained as described in chapter 2. Once the correct tagged *emrE* gene sequence was confirmed by DNA sequencing, C43(DE3) cultures containing the tagged EmrE plasmid, pTZemrEmH6, were assayed to determine the conditions necessary for protein accumulation in the membrane in preparation for batch cell culture. Thus, two questions were addressed in the following studies to ensure that 1.) the expression system resulted in accumulation of tagged EmrE in the bacterial membranes and 2.) the cell culture reaches mid-log phase in a reasonable amount of time and also reaches a suitable mass for harvesting of the cells. The first point was addressed by performing a dot blot assay comparing induced and uninduced cultures. The second point was addressed by recording time-point cell densities to construct a growth curve comparing cells containing the tagged *emrE* plasmid and cells containing an empty vector.

4.1.1 Dot blot assays

Tagged *emrE* expression, as alluded to earlier, requires induction using isopropyl-β-D-1-thiogalactopyranoside (IPTG). Too much or too little IPTG is detrimental to protein purification as too much could lead to toxic effects of the expressed membrane protein and too little could result in a low protein yield. It was also important to determine if IPTG would induce accumulation of the tagged EmrE at all.

4.1.2 Results

Spots that developed color were expected to correspond to where the His_6 specific antibody had bound. Overall, cultures accumulated the most tagged EmrE protein 3 hours after IPTG induction (figure 3.1). There is an observable increase in tagged EmrE concentration over the 3 hours after IPTG induction for cultures induced with 0.3 and 0.5 mM IPTG whereas there was little change over time with cultures induced with 0.1 mM IPTG. Spot intensities between cultures induced at 0.3 and 0.5 mM IPTG 3 hours after induction were comparable. Cultures of C43(DE3) cells containing the pTZ6HmErmE (encoding a nonsense mutation without a 6 histidine sequence in the multiple cloning site), did not develop color on the dot blot. On the other hand, TatA-*myc*-His_6 did develop a colored spot indicating that the INDIA HisProbe-HRP antibody specifically bound 6 histidine sequences (figure 3.1). Uninduced cultures that were spotted on the membrane bound antibody indicating the presence of "leaky" expression of the pTZEmrEmH6 plasmid leading to the production of some amount of tagged EmrE.

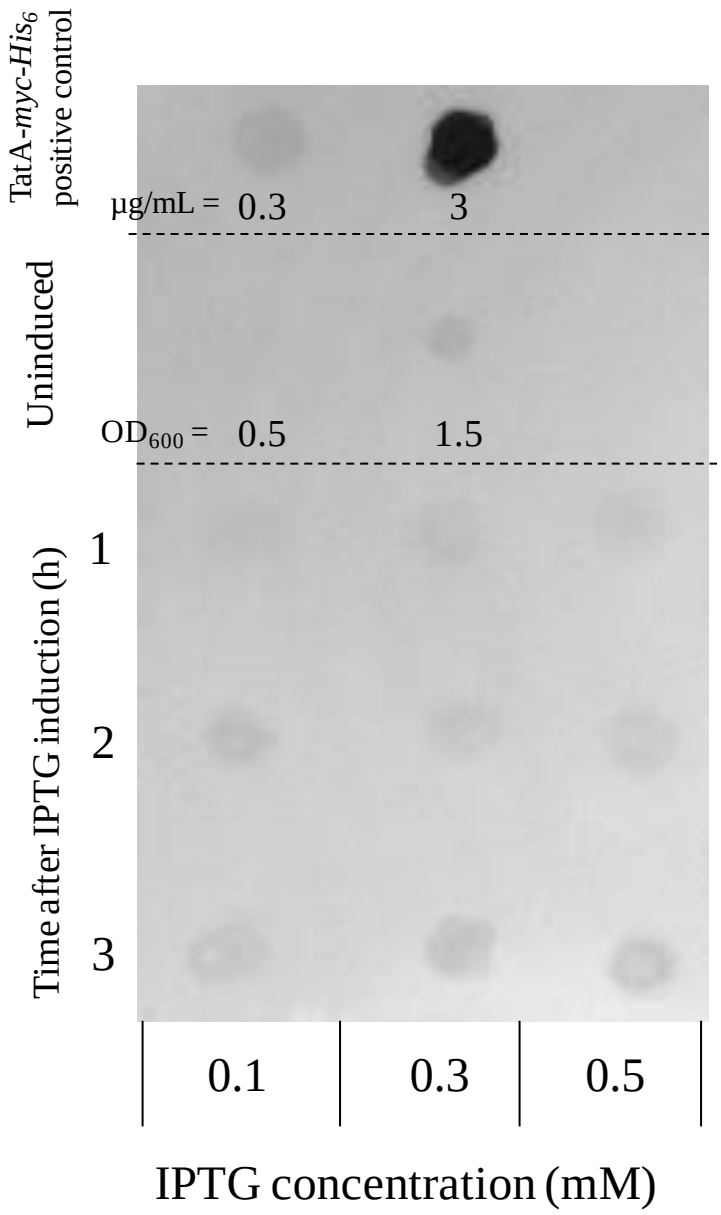

Figure 3.1: Dot blots of C43(DE3) + pTZEmrEmH6 cultures spotted onto a nitrocellulose membrane induced with 0.1, 03, or 0.5 mM IPTG. Membrane was blotted in a solution of the 6-hisitdine specific anti-body INDIA HisProbe-HRP (5 µg/mL). Cell cultures collected 1, 2, and 3 hours after IPTG induction were spotted on the membrane. TatA-myc-His_6 was included as a positive control for the antibody. Uninduced cultures also developed color indicating the presence of tagged EmrE.

4.1.3 Growth curves

Overexpression of membrane proteins have been known to be lethal even though the C43(DE3) strain contains two mutations that improve the expression in these cases (Miroux and Walker, 1996). As a preliminary to batch culture, cells containing the tagged *emrE* gene were cultured and compared to cells containing empty vector in order to optimize protein yield.

4.1.4 Results

The aim was to have a cell culture that could reach mid-log phase near 4-5 hours and an OD_{600} = 1, 3 hours after induction with IPTG. This was to ensure that cells could be cultured and harvested within a reasonable amount of time during a work day. Growth curves were constructed from 3 replicate data sets (figure 3.2). The C43(DE3) + PTZEmrEmH6 cultures reached mid-log phase around 4.5 hours after inoculation and the final OD_{600} was around 1 after 7.5-8 hours of growth. Furthermore, the growth was comparable to cultures containing the empty vector in place of the tagged *emrE* plasmid indicating minimal toxic effects.

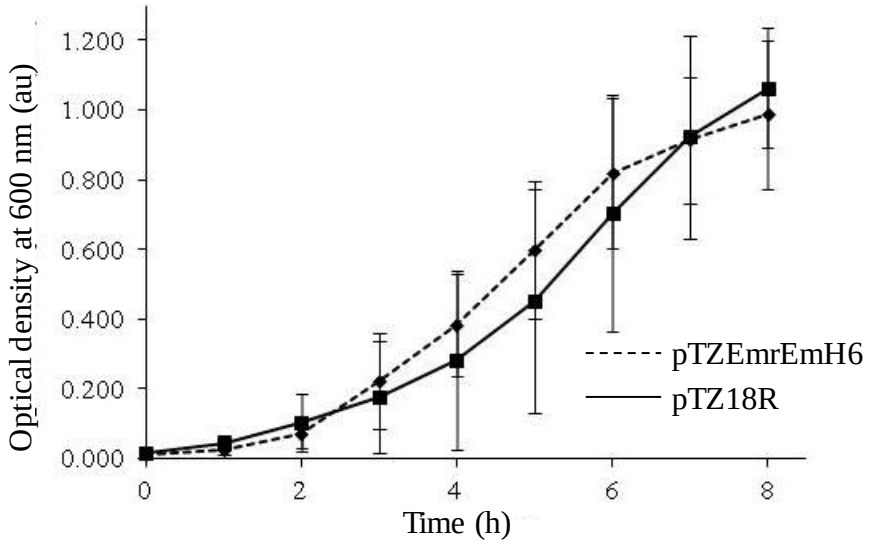

Figure 3.2: Growth curve of C43(DE3) cells containing either the pTZEmrEmH6 or pTZ18R plasmid.

4.2 SDS-Tricine PAGE analysis of purified EmrE

Chromatography fractions were analyzed using 12% T SDS-Tricine PAGE to confirm the presence of untagged and tagged EmrE from respective preparations. An SDS-Tricine PAGE method (Schagger, 2006) was selected over conventional SDS-PAGE as EmrE was expected to have a monomer molecular weight of less than 30 kDa. The main difference between the two techniques is the electrophoresis buffer used: glycine-Tris and tricine-Tris. Using the tricine-Tris buffer was expected to result in better separation of proteins that are in a range of less than 30 kDa due to the pKa of Tricine, the trailing ion (Schagger, 2006).

4.2.1 Results

Multiple bands were observed in both EmrE lanes corresponding to different oligomer forms (figure 3.3). Additionally, a single band below either molecular weight was also observed consistent with different redox states of EmrE (Winstone *et al*., 2002). Thus, each preparation resulted in the purification of the expected proteins and both procedures resulted in a mixed population of oxidized and reduced EmrE. The corresponding yields to each EmrE preparation are shown in table 3.1.

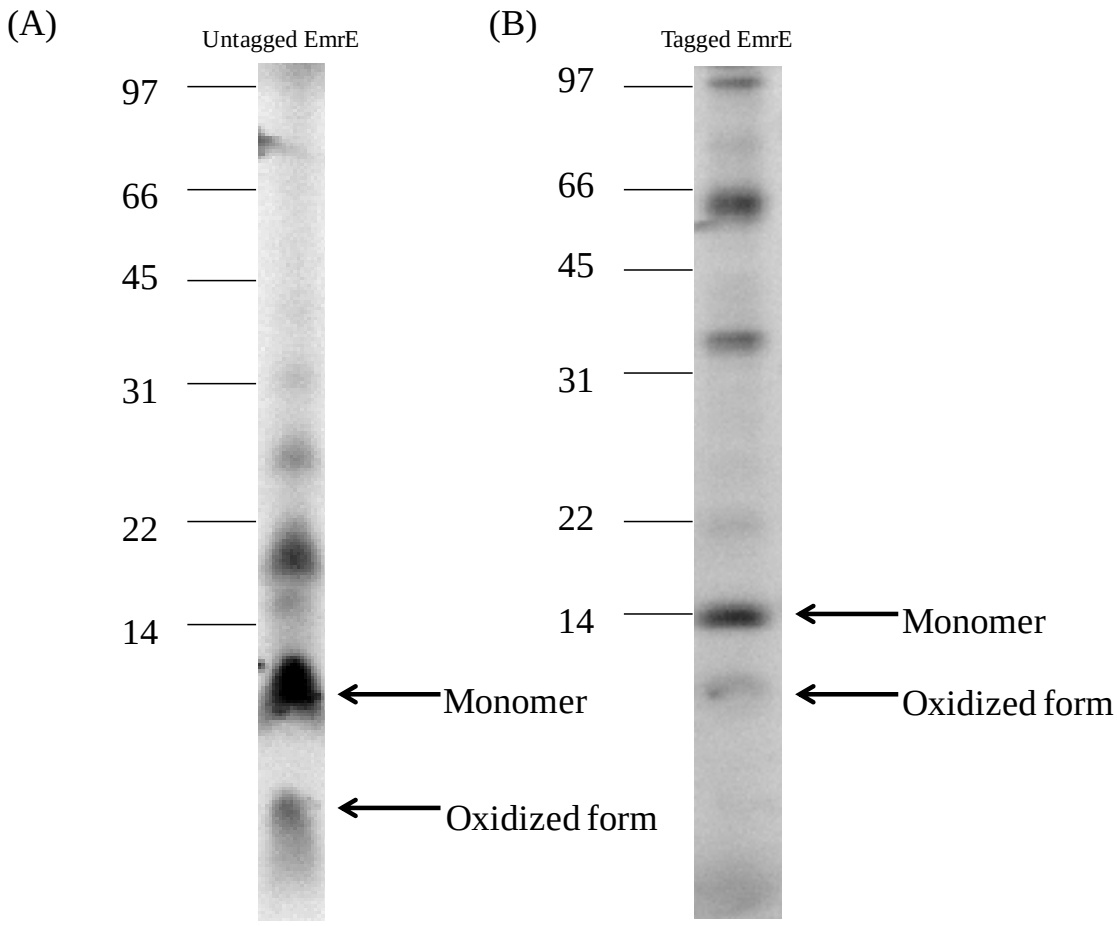

Figure 3.3: Undiluted EmrE samples after respective isolations of (A) untagged EmrE and (B) tagged EmrE on a 12% T SDS-Tricine PAGE. Bands were visualized under UV after incubating gels in a 0.1% v/v TCE solution for approximately 15 minutes.

Table 3.1: Yields of Untagged and Tagged EmrE from respective isolations

	μmol protein / L of culture	
EmrE:	Lower limit	Higher limit
Untagged	0.00056	0.00067
Tagged	0.00283	0.00517

4.3 EmrE solubilisation and concentration determination

Tagged EmrE samples did not require further treatment after elution from the HiTrap desalting column directly equilibrated with DDM buffer. On the other hand, untagged EmrE needed to be solubilised in the same buffer for a valid comparison. Untagged EmrE samples stored at -20°C were solubilised DDM buffer (20 mM Tris-HCl, pH 7.5, 100 mM NaCl, 0.08% w/v DDM). 300 μL of the DDM buffer was added to each micro-centrifuge tube containing the dried down untagged EmrE protein powder and the sample was placed in a plastic beaker of water. The water was then sonicated using a Misonix probe-type sonicator. To avoid contamination from the probe tip, samples were not sonicated directly. This was repeated 3 times at 10 minute intervals. The sonicated sample was then centrifuged in an eppendorf 5417C table-top centrifuge for 1 minute at 10,000 x g to remove un-solubilised material. A non-centrifuged untagged EmrE sample was also obtained for comparison. Both centrifuged and non-centrifuged samples started from identical solvent-evaporated EmrE amounts.

4.3.1 Protein concentration determination

Typically, colorimetric assays such as the Bradford assay and Lowry assays are useful for the determination of protein concentration. These assays are not amenable for membrane proteins that require solubilisation in a detergent containing buffer. Coomassie blue, the dye used in Bradford assays, is hydrophobic and can bind to amphiphilic surfactants found in solubilised membrane protein samples leading to overestimation of protein concentration. Lowry assays and modified Lowry assays have limited ranges of detection and are not sensitive to EmrE samples that become solubilised at low concentrations. Fortunately, a sensitive determination method exists by absorbance measurements if the molar extinction coefficient for a protein can be calculated. The molar extinction coefficient at 280 nm for untagged EmrE is 29450 $M^{-1}cm^{-1}$ and 30940 $M^{-1}cm^{-1}$ for tagged EmrE as calculated using the following equation from Gil and von Hippel (1989):

$$\varepsilon_{protein} = n_{Trp} * \varepsilon_{Trp} + n_{Tyr} * \varepsilon_{Tyr} + n_{cystine} * \varepsilon_{cystine} \quad (1)$$

Where $\varepsilon_{protein}$, ε_{Trp}, ε_{Tyr}, and, $\varepsilon_{cystine}$, are the extinction coefficients of the protein, Trp (5500), Tyr (1490), and cystine (the cysteine disulfide; 125), respectively in the units of $M^{-1}cm^{-1}$. "n" is the number of Trp, Tyr, or cystines found in the protein. Under native conditions, untagged EmrE contains 4 tryptophans, 5 tyrosines, and 0 cystines. Tagged EmrE differs by having 6 tyrosines (see figure 1.4)

Though the use of absorbance is a sensitive measure, scattering effects from detergents can lead to perturbation of spectral data. Initially, absorbance spectra of each

EmrE sample were collected using Ocean Optics UV-visible Spectrophotometer. This spectrophotometer is capable of not only single wavelength absorbance, but also reading absorbances across a range of wavelengths. Recording the absorbance at a single wavelength, such as 280 nm, is insufficient to observe spectra effects of scattering, a common effect among solutions containing detergents due to micelle formation. The absorbance spectrum between 220 nm to 300 nm was recorded for each EmrE sample. A 1 cm path length quartz cuvette was used for each measurement with about 300 µL of sample. Tagged EmrE samples were diluted ½ from stock solutions due to generally high absorbance signals. A further ½ dilution was prepared as an internal control to see if protein concentrations affect signal from light scatter. Undiluted untagged EmrE samples from the DDM solubilisation were also compared with itself at ½ dilution. All dilutions were made in DDM buffer.

4.3.2 Absorbance results

An expected protein absorbance spectra would have a maxima around 270-280 nm due to the absorbance of the intrinsic chromophores, tyrosine (Tyr) and tryptophan (Trp). Absorbance was observed in this region for both untagged and tagged EmrE, however, only the tagged EmrE had an absorbance maxima (figure 3.4). Untagged EmrE absorbance spectra peaks were not as prominent. Furthermore, there was significant signal at 300 nm, a wavelength that proteins generally do not absorb. The non-protein absorbance was present in both EmrE samples, despite subtraction of the 0.08% w/v DDM buffer was from each absorbance spectrum. Although reliable protein

concentrations could not be determined from this data, there was an observed difference between untagged and tagged EmrE in terms of the extent of scattering effects.

4.3.3 Identifying the source of light scattering

Light scattering is due to the presence of large particles relative to the wavelength of light being used. Instead of being absorbed, light is reflected by the particles and does not reach the detector in standard spectrophotometers. To determine if the large particles of EmrE were due to insoluble material forming aggregates, an untagged EmrE sample that was not centrifuged during solubilisation was compared to a sample that was centrifuged.

4.3.3.1 Results

The intensity of untagged EmrE absorbance decreased and the amide peak with a maximum near 230 nm was more prominent after centrifugation (figure 3.4A and C). Centrifugation of untagged EmrE after sonication in DDM buffer resulted in a visible pellet. When loaded onto a gel, only a single band corresponding to the monomer molecular weight appeared in the centrifuged untagged EmrE lane (figure 3.5). As for the untagged EmrE that was not centrifuged, dimeric and trimeric migrations were observed and the overall intensity of the bands was much darker. A reduction by 86% in protein concentration was calculated from the band intensities of the centrifuged and non-centrifuged samples.

4.3.3.2 Discussion

Centrifugation helped to decrease the influence of scattering effects on the absorbance spectra. A visible peak maxima between 270 and 280 nm was not observed, however. Oligomerization is a concentration dependent phenomena and it was consistent that the non-centrifuged samples formed oligomers due to it being 6 times more concentrated. Despite the disparity in concentration, the centrifuged sample was chosen for future assays due to the reduced amount of insoluble material apparent from the absorbance spectra comparison.

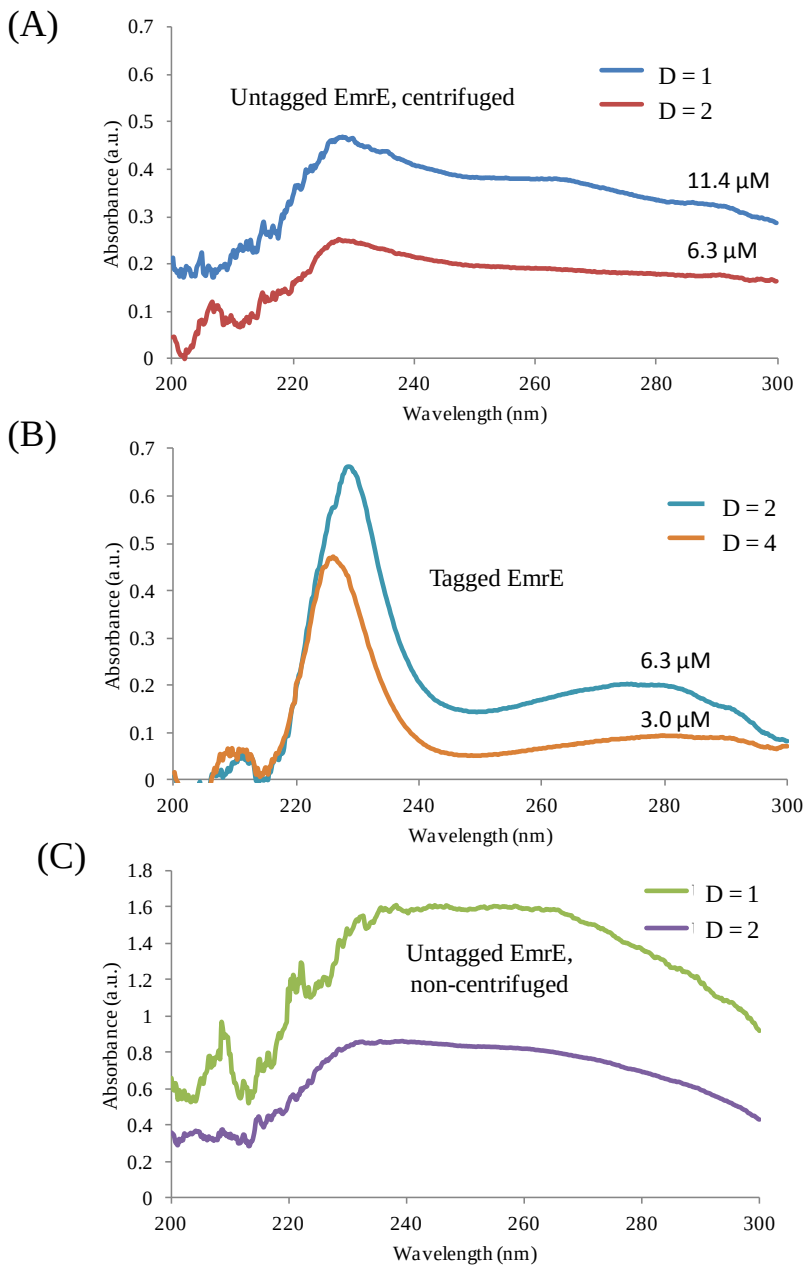

Figure 3.4: Absorbance spectra of untagged EmrE and tagged EmrE. Each sample was diluted according to the indicated dilution factor "D", to compare concentration effects on the absorbance spectrum. (A) Untagged EmrE sample that were solubilised in DDM buffer and centrifuged to remove insoluble material. (B) Tagged EmrE sample eluted from the HiTrap-desalting column. Concentrations of A and B corresponding to each spectra were calculated using the estimated molar extinction coefficients and the absorbance at 280 nm. (C) Untagged EmrE that was not centrifuged during the solubilisation step.

4.3.4 Discussion

Detergents in membrane protein solutions can cause scattering. Both types of EmrE were solubilised in a 0.08% w/v DDM solution, a concentration nearly 10 times the critical micelle concentration (CMC) (~0.009% w/v in water for DDM). A likely cause for the observed difference in scattering could be the solubilisation conditions experienced by each EmrE. Beginning from the membrane extraction, untagged EmrE was exposed to chloroform : methanol organic solvent solutions until its elution from the size exclusion column. At this point, the protein was solvent-evaporated and required an addition solubilisation step into DDM buffer. Unlike its untagged counterpart, tagged EmrE was equilibrated with solutions containing DDM beginning from membrane extraction and only the DDM concentration was decreased stepwise from 4% w/v to 0.08% w/v. Tagged EmrE encountered more chances to equilibrate with DDM micelles than untagged EmrE did during the respective purifications. The untagged EmrE solution contained more scattering components that interfered with the protein absorbance signal.

4.3.5 Protein concentration determination by band intensities on a SDS-Tricine PAGE

SDS-Tricine PAGE can give concentration information using the staining method described in section 2.3. The lysozyme band of the Bio-Rad Low molecular weight protein standards was used as a known concentration of protein. Lysozyme has a molecular weight similar to EmrE and also shares the common feature of possessing 4 tryptophan residues. Assuming that all the tryptophans react with TCE in the staining solution, the EmrE concentrations can be estimated by corresponding the intensity of the EmrE bands to the lysozyme band. TCE-stained gels were imaged using a KODAK Gel-

Logic 100 Imaging System. Lanes and bands were selected and adjusted using the KODAK 1-D application. For each lane selected, a non-band area was selected for estimation of background intensity. Bio-Rad Low molecular weight protein standards were loaded into the gel at 2 concentrations to ensure that the band intensities corresponded to relative concentration change. Two types of untagged EmrE samples were loaded into the gel: one that was centrifuged during the solubilisation and one that lacked the centrifuge step (see section 2.4).

4.3.5.1 Results

Estimations of concentrations by band intensity on a PAGE gel were lower than the values estimated using absorbance at 280 nm. Untagged EmrE was nearly 30 times higher when estimated using A_{280} values whereas tagged EmrE was nearly 6 times higher (figure 3.5). Multiple bands appearing in the EmrE lanes were accounted for by a sum of each band intensity-measured concentration to get a value for the total EmrE content.

4.3.6 Discussion

Estimation of relative protein concentrations using TCE stained PAGE gels have been shown to be reproducible and accurate (Ladner *et al.*, 2004). The tryptophans of the reference lysozyme and the tryptophans in the EmrE were assumed to have reacted with the TCE in the same relative molar ratios. The same was also assumed for the higher order oligomers of EmrE. Compared to determination by absorbance, the band intensity analysis fortunately does not encounter interference from scattering due to micelle-protein bodies. Furthermore, higher order oligomeric EmrE forms that may also cause

scatter in absorbance spectra are quantified on the TCE-stained gel. Thus, protein concentration-sensitive assays used in this study were quantified by this method.

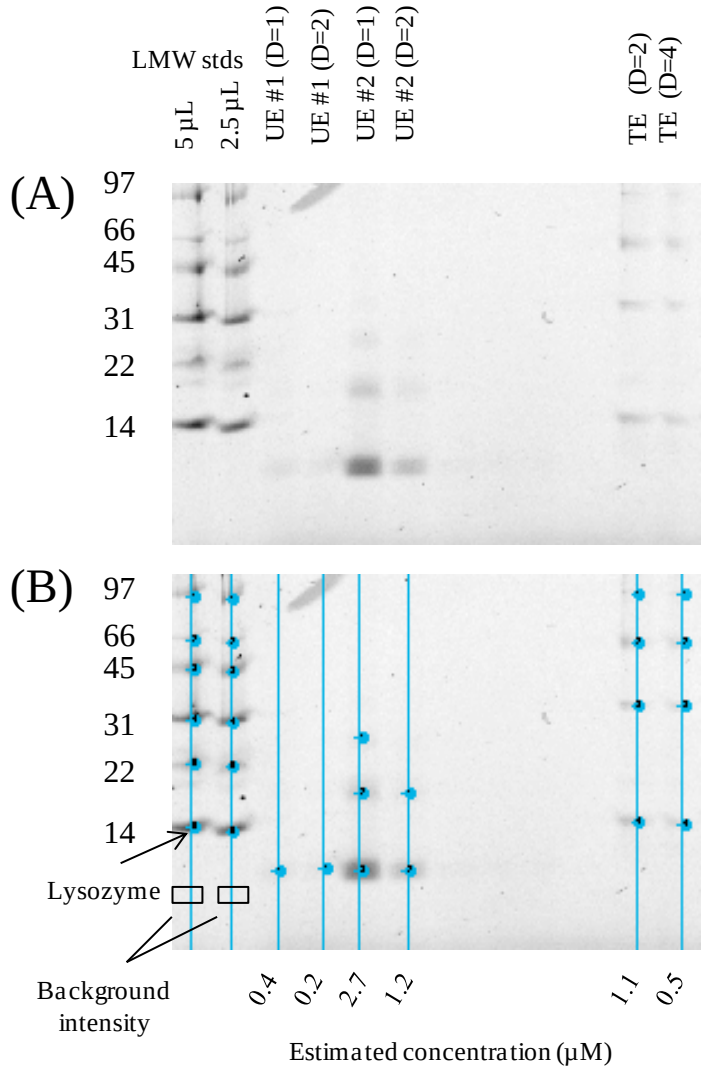

Figure 3.5: (A) SDS-Tricine PAGE of EmrE samples. Gel was stained using 2,2,2-trichloroethanol (TCE). Abbreviations: UE is untagged EmrE, TE is tagged EmrE, LMW stds is the BioRad Low molecular weight protein standard. UE#1 was centrifuged during the solubilisation step whereas UE#2 was not. (B) is the same image of the TCE-stained gel but lanes and bands have been located using the KODAK 1-D application, from the band intensities and the known lysozyme concentration, the total protein concentrations in each lane were calculated.

Chapter Five: **Fluorescence Spectroscopy**

5.1 Fluorescence spectra

The fluorescence spectra of untagged and tagged EmrE provided information about protein folding. Fluorescence occurs when a particle (fluorophore) absorbs light to reach an excited singlet state and upon relaxation to the ground state, a photon is emitted. The emission wavelength is typically longer than the excited wavelength, a phenomenon known as the Stokes shift. Additionally, the fluorescence intensity of solvent-exposed molecules may also be lower. The behavior of the nearby solvent molecules forms the basis of this shift and intensity change. As the local environment around the fluorophore increases in polarity, the emission maximum can be observed at longer wavelengths from the excitation. Re-orientation of the solvent around the fluorophore and bond vibrational relaxation results in some energy dissipation, hence the longer emission wavelength and lower intensity. Less polar solvent molecules tend not to re-orientate as drastically in response to a change in the electron distribution of the fluorophore (Lakowicz, 2006). Tryptophans and tyrosines in proteins are fluorophores that act as molecular sensors to solvent polarity. The sidechains of these two residues contribute the most to the fluorescence of a protein due to delocalized electrons in aromatic rings that contain photon inducible dipole transitions. Fluorescence can be used to map the general location of these residues on the protein. When these aromatic side chains are buried deep within the protein fold, the Stoke's shift is not as dramatic due to the relative hydrophobic environment.

Both untagged and tagged EmrE contained 4 tryptophans, but there were 5 tyrosines in untagged EmrE and 6 in the tagged version. In order to make a proper

comparison, only the tryptophans were excited by using a 295 nm excitation, a wavelength at which tyrosines do not absorb. Trp63 located in the EmrE binding pocket has been observed to be important for ligand binding as mutation at this position abolishes binding (Yerushalmi *et al.*, 1996; Elbaz *et al.*, 2005). There are two more tryptophans within transmembrane segments 2 and 3 while the remaining tryptophan can be found in loop 2. Samples of untagged and tagged EmrE in DDM buffer were assayed at a concentration of 10 nM. The fluorescence emission spectra were collected and compared.

5.2 Results

Relatively, untagged EmrE displays more internal quenching than did the tagged EmrE (figure 4.1). The protein concentrations were determined to be the same by calculations based off the absorbance at 280 nm. At the same concentrations, the fluorescence emission of the tagged EmrE was consistently more intense than the untagged EmrE. Both untagged and tagged EmrE spectra had an emission maximum (λ_{max}) at 338 nm. However, there was another peak of comparable magnitude with λ_{max} at 328 nm in the tagged EmrE emission spectra.

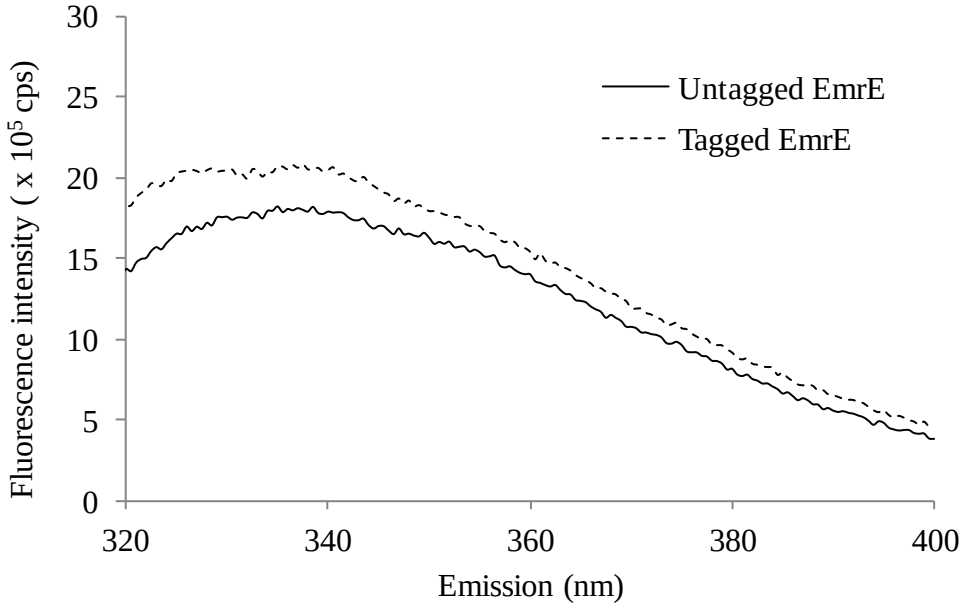

Figure 4.1: Fluorescence emission spectra of 10 nM untagged and tagged EmrE in DDM buffer.

5.3 Discussion

The emission maximum at 338 nm for both EmrE types is consistent with previous observations at 340 nm (Elbaz *et al.,* 2005). Two emission maxima observed in the tagged EmrE spectra indicate the presence of 2 different states of tagged EmrE. The 328 nm emission maxima were particularly unusual as it represented the tryptophan in a relatively more hydrophobic environment. There are 3 transmembrane tryptophans that are found in helices 2 and 3 of EmrE that can be affected by packing of the protein. It is possible that the peptide tag can adopt a conformation in close proximity to these tryptophans and displace nearby solvent molecules. An interaction between the hydrophilic affinity tag and the hydrophobic core of EmrE is unlikely. Recently, the single-site alternating access model for membrane protein transporters (Jardetsky, 1966) has been adopted for EmrE (Fleishman *et al.,* 2006; Henzler-Wildman, 2012). According to this model, access to the single EmrE binding site is formed from an anti-parallel dimer and access is controlled by 2 flexible loop regions between transmembrane 3 and 4. In a bilayer setting, there is one flexible loop on either side of the membrane due to an anti-parallel topology. Furthermore, a transient water-occluded state is thought to exist between the opening of the binding site from one side of the bilayer to the other (Basting *et al.,* 2008; Lehner *et al.,* 2008). Stabilization of this state either from the purification procedure or the peptide tag could result in a more hydrophobic environment of binding site tryptophans. Untagged EmrE was purified in organic solvent which could have dissociated this transient water occluded state.

Chapter Six: **Red-edge excitation shift**

6.1 The REES effect

The fluorescence emission is typically independent of the excitation wavelength due to the rapid relaxation of surrounding solvent molecules relative to the time the fluorescent molecule spends in the excited state. However, in a more viscous solvent environment where solvent relaxation is slow, a fluorophore can display a property known as the REES (red-edge excitation shift) effect (Lakowicz, 2006). In an extreme case of viscosity, a frozen solution contains solvents in a fixed configuration about the fluorophore. By chance, some of these fluorophores have solvent configurations resembling a relaxed state and form hydrogen bonds with the solvent. As a result, less energy is required for excitation and the emission is red-shifted (see figure 5.1). These longer excitation wavelengths are known to be on the "red-edge" of the molecule's absorption range. Tryptophans and tyrosines in proteins can be found in relatively more "viscous" conditions than in free solution due to structure and folding that can restrict the re-orientation of solvent. Excitation with red-edge wavelengths can select for emissions of fluorophores in a solvent-restricted environment. At least 1 tyrosine (Tyr40) and 1 tryptophan (Trp63) are located in the binding site of EmrE (Sharoni *et al*., 2005). Furthermore, the emission spectrum of EmrE is heavily influenced by Trp63 (Elbaz *et al.,* 2005). A red-shifted emission can be the result of interactions of these fluorophores with nearby protein residues in the binding cavity of EmrE. In combination, the absorption ranges of tyrosine and tryptophans begin at around 305 nm and ends at 260 nm. This technique was used to probe the relative dynamics of the fluorophore environment within untagged and tagged EmrE in DDM buffer.

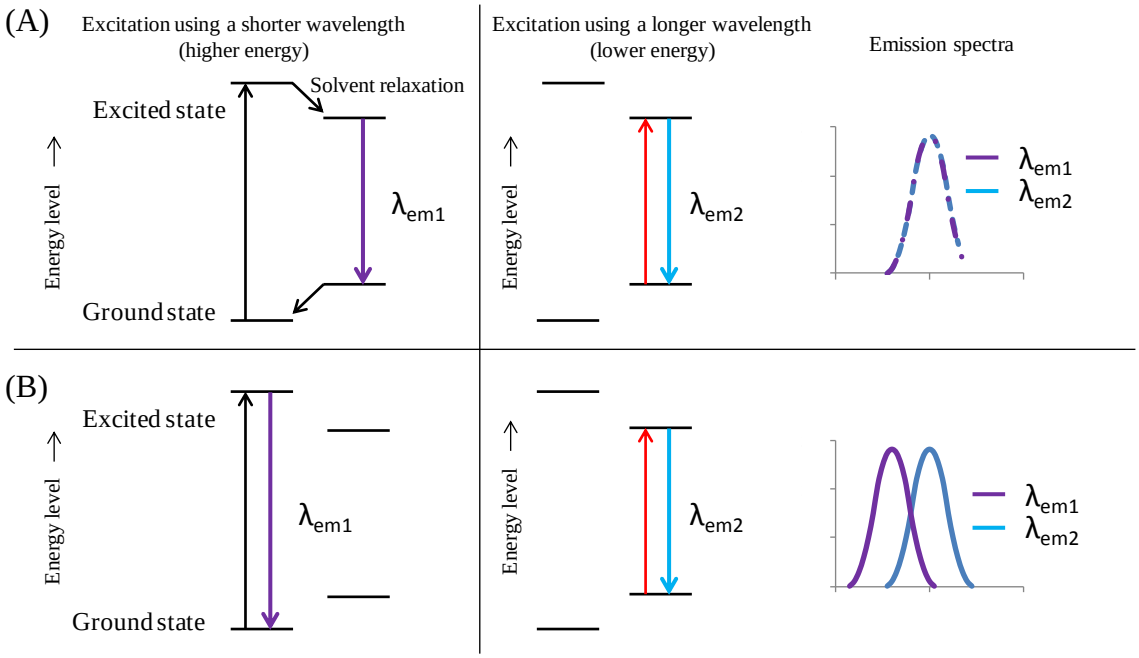

Figure 5.1: Jablonski diagrams illustrating the REES effect. (A) When solvent relaxation is faster than the emission of photons, the emission spectra is independent of the excitation wavelength used. (B) Conversely, when the solvent relaxation is slower than the emission of photons, a red-shifted emission spectra is observed when a lower energy wavelength is used for excitation.

6.2 Results

There was a marked difference between the behaviour of untagged and tagged EmrE fluorescence emission spectra in response to the excitation wavelength used. A peak with a λ_{max} of 332 nm was observed in untagged EmrE samples at all excitation wavelengths used (figure 5.2 and 5.3). However, a second peak at approximately 348 nm was apparent when a 290 nm or longer excitation wavelength was used. In contrast, tagged EmrE emission spectra were of a comparable shape with a λ_{max} between 332-336 nm across all excitations except for 305 nm. Changes between the 332-336 nm range did not display any particular trend with respect to the excitation wavelength used and were largely attributed to noise rather than to solvent dynamics. At 305 nm, a red-shifted emission with a λ_{max} of 342 nm was observed. Only 1 peak was identified for tagged EmrE at all excitations whereas 2 peaks were observed for untagged EmrE depending on the excitation wavelength used.

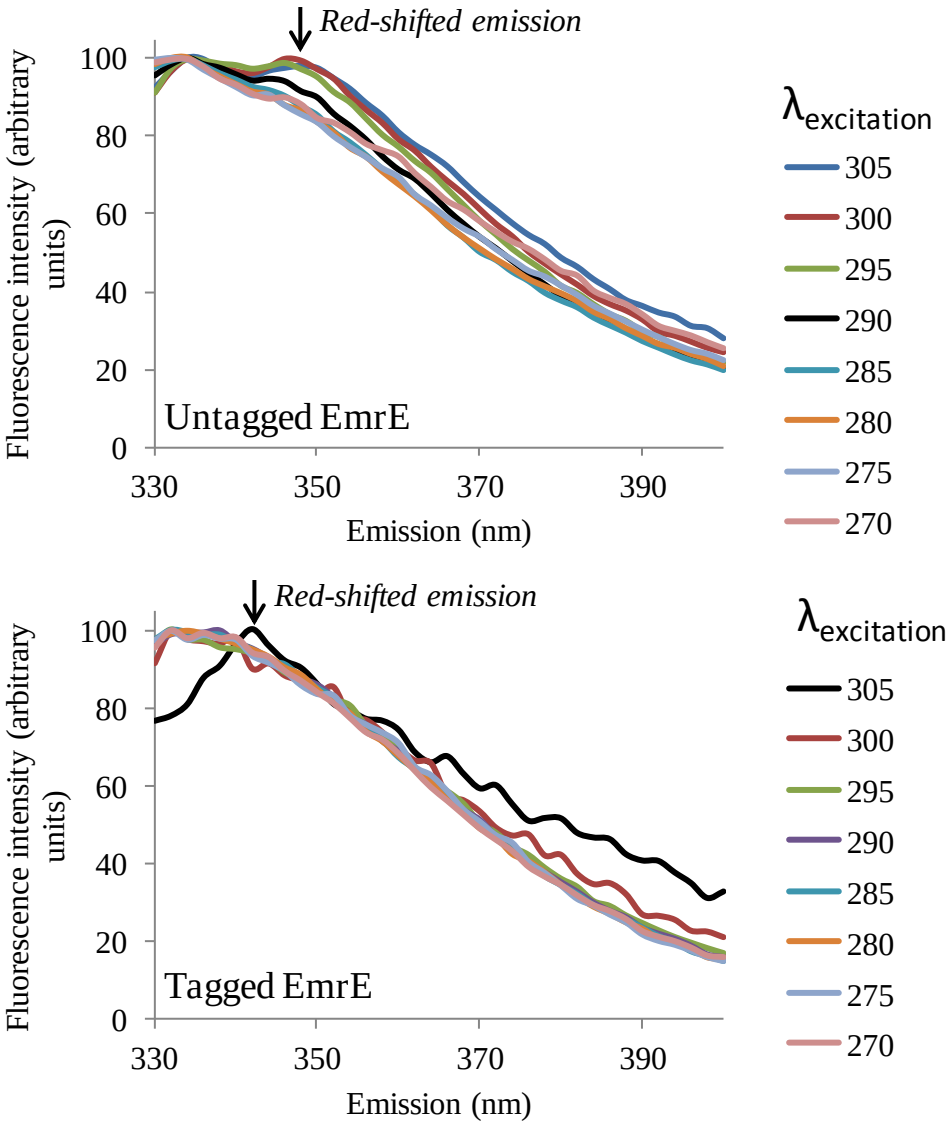

Figure 5.2: Raman-subtracted fluorescence emission spectra of untagged (top) and tagged EmrE (bottom) collected using different excitation wavelengths ($\lambda_{excitation}$). All spectra were normalized to have a maximum intensity of 100% for comparison of the peak positions.

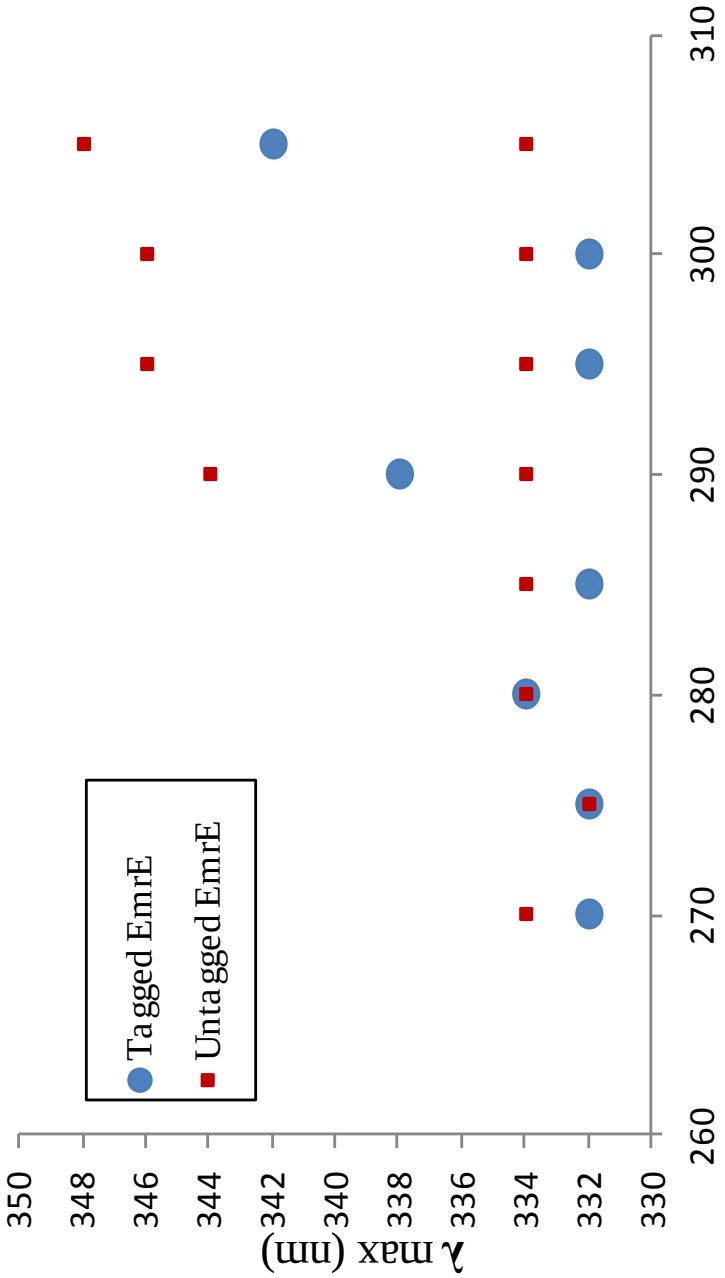

Figure 5.3: REES plot of excitation wavelength versus emission maximum. Untagged EmrE has 2 emission peaks of similar magnitudes when the sample was excited at 290, 295, 300, and 305 nm.

6.3 Discussion

Structure plays a large role in the solvent dynamics of EmrE. The purification process to obtain EmrE can affect dynamics by influencing solubilisation conditions (Federkeil *et al.*, 2003) and also by affecting the oligomerization state (Elbaz *et al,* 2005; Winstone *et al,* 2004). The red-shifted emission observed for the tagged EmrE reflects an environment that restricts solvent re-orientation. This indicates that the tryptophans are in a "viscous" environment that restricts conformational freedom. In contrast, the untagged EmrE conclusions were not as straightforward. A red-shifted emission peak was observed for untagged EmrE, however, the emission at 332 nm did not disappear as expected in a classical REES effect. Longer wavelengths do not have enough energy to overcome the unfavorable interactions of excited state tryptophans with conformationally restricted solvent molecules. This puzzling characteristic can be explained if some of the tryptophans can absorb the lower wavelength light and transition to a higher electronic energy level. In fact, this phenomenon is known as reverse relaxation (Lakowicz, 2006). Reverse relaxation occurs when the emission lifetime is comparable to the lifetime of solvent relaxation (Nemkovich *et al.*, 1979). At first glance, solvent relaxation to the higher electronic energy level in the excited state seems unfavorable (figure 5.4). However, the total free energy may be low due to the favorable conformational energy of the tryptophan and its surrounding molecules. In the case of untagged EmrE, the 332 nm peak can be due to reverse-relaxation of the solvent for samples excited at the long wavelengths. Taken together, these findings suggest that the tryptophans in untagged EmrE are in an environment with quicker solvent dynamics than the tryptophans in

tagged EmrE. A more compact environment can be formed from the tag interfering with oligomerization, packing of the helices, or interactions of the tag directly with the binding site. Within these interfaces and cavities, nearby amino acid residue side-chains play the role of the “solvent” that do not re-orientate easily due to covalent bonds and steric hindrances within the folded protein. The environment around untagged EmrE tryptophans is more dynamic.

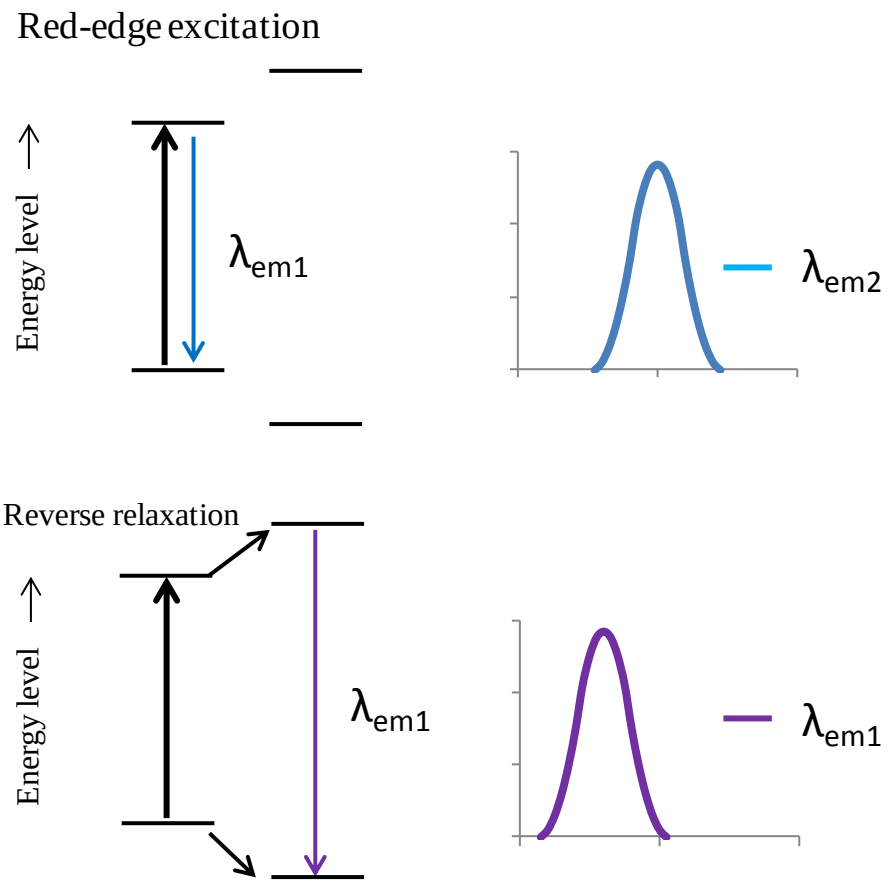

Figure 5.4: Jablonski diagram illustrating effects of reverse relaxation of solvent to a higher electronic energy level (bottom). The top figure shows the behavior of the emission in the absence of solvent reverse-relaxation.

Chapter Seven: **EmrE-Ligand binding**

7.1 Background

The functionality of the untagged and tagged EmrE was compared *in vitro* by examining ligand binding. Ligand binding curves can be constructed by plotting quantifiable changes specific to the binding protein against ligand concentration. The quantifiable property in this case is the EmrE tryptophan fluorescence intensity. Ligand binding was followed by observing the fluorescence changes of EmrE in response to a titration of the QCC: Eb, MV, CTPC, or TPP. A comparison of untagged and tagged EmrE was possible due to the same amount of tryptophan (Trp) in both proteins. Though untagged and tagged EmrE differ in the amount of the intrinsic chromophore tyrosine (Tyr) (5 in untagged and 6 in tagged EmrE), there are 4 Trp residues in both proteins that can be followed using fluorescence. Thus, a 295 nm excitation was used to select only for Trp as Tyr does not absorb at this wavelength. The EmrE active site has been observed to contain a single Trp at position 63 (Elbaz *et al.*, 2005; Sharoni *et al.*, 2005), although there are also 2 Tyr residues in the active site at positions 4 and 40 (Sharoni *et al.*, 2005; Rotem *et al.*, 2006). Changes in the fluorescence intensity can be tracked at a constant emission wavelength and plotted against Eb, MV, or CTPC concentrations to obtain a binding curve. The dissociation constant (K_D) can be calculated from this type of plot and is indicative of the affinity of a protein to a ligand. Differences in the K_D between untagged and tagged EmrE was compared to get an idea of the equivalence of the respective purification protocols. For this purpose, inner filter effects were intentionally not considered during the calculations as both untagged and tagged EmrE were titrated with identical ligand concentrations. Inner filter effects occur when an added compound

interferes with the spectral measurement of the compound of interest by absorbing light at the incident wavelength. This would prevent a fraction of the incident light from reaching the absorbing species of interest. Thus, a decrease in the emission intensity due to a decrease in the amount of incident light absorbed is incorporated into the experimental data. However, the amount of light reaching the untagged and tagged EmrE during the respective ligand titrations should be the same as both proteins were titrated identically.

To date, EmrE ligands belong to a class of compounds, the quaternary cationic compounds, that all contain at least one positively charged atom that have 4 electrons participating in 4 bonds with R groups. Various ligands have been previously shown to bind untagged EmrE whereas the TPP^+ ligand has been primarily used to test binding with tagged EmrE (table 6.1).

Table 6.1: Binding affinities of QCC to EmrE evaluated under different conditions

(A) Tagged EmrE**

Assaying condition	Experiment	Ligand	K_D (μM)	Standard deviation	Reference
0.08% w/v DDM	Equilibrium dialysis	[^{3}H] TPP	0.01	0.003	Muth and Schuldiner, 2000
0.8% w/v DDM	Saturation binding assay	[^{3}H] TPP	0.0028	0.001	Rotem et al, 2001
0.1% w/v DDM	Saturation binding assay	[^{3}H] TPP	0.0026	0.4	Tate et al, 2003
0.5% w/v DDM (delipidated EmrE)	Saturation binding assay	[^{3}H] TPP	2.5	0.5	Butler et al, 2004
0.5% w/v DDM (non-delipidated EmrE)			10	2	

(B) Untagged EmrE

Assaying condition	Experiment	Ligand	K_D (μM)	Standard deviation	Reference
SUV	ITC	EtBr	5.5	2.1	Sikora and Turner, 2005
		MV	38.2	8.7	
		Pro	10.7	2.7	
8% w/v SDS	ITC	EtBr	5.2	1.4	
		MV	5.4	1.2	
		Pro	4.5	0.8	
		TPP	4.8	0.8	
2% w/v DDM	ITC	EtBr	6.3	1	
		MV	46.2	10.5	
		Pro	5.2	0.9	
		TPP	25.5	6.2	
2% DDM	Fluorescence	EtBr	6.81	0.53	Winstone et al, 2004
		MV	43.6	3.8	
		Pro	23.6	7.1	
		CTP	6.61	2.2	

*Abbreviations in first column: QCC = quaternary cationic compound, DDM = *n*-dodecyl-D-β-maltoside detergent; SUV = small unilamellar vesicle from E. coli polar lipid extracts; SDS = sodium dodecyl maltoside detergent. Second column: ITC = Isothermal titration calorimetry. Third column: [^{3}H] TPP = tritium labelled tetraphenylphosphonium; EtBr = ethidium bromide; MV = Methyl viologen; Pro = Proflavin; CTP = cetylpyridinium chloride.
**Tagged EmrE and untagged EmrE sequences differ by an additional C-terminal *myc*-epitope, and 6-histidine peptide tag.

Subtle differences in the structure of untagged and tagged EmrE could affect the affinity for different ligand shapes. Thus, the 3 QCC selected were each selected based on varying structural themes (figure 1.3). Ethidium was selected based on its flat planar structure, methyl viologen was selected based on its 2 cationic charges, and cetylpyridinium was chosen because it had a long alkyl chain with its overall structure reminiscent of a surfactant molecule.

7.2 Results

7.2.1 Baseline corrections

The DDM buffer had an emission spectrum when a 295 nm excitation was used (see figure 6.1). Moreover, the fluorescence intensity decreased as more ethidium was titrated into solution. To correct for the different blank solution intensities at each ethidium concentration, the signal contribution was simply subtracted from the corresponding EmrE-ligand titration at each ligand concentration. Similar effects were seen with MV and CTPC: spectral data were corrected in an identical manner.

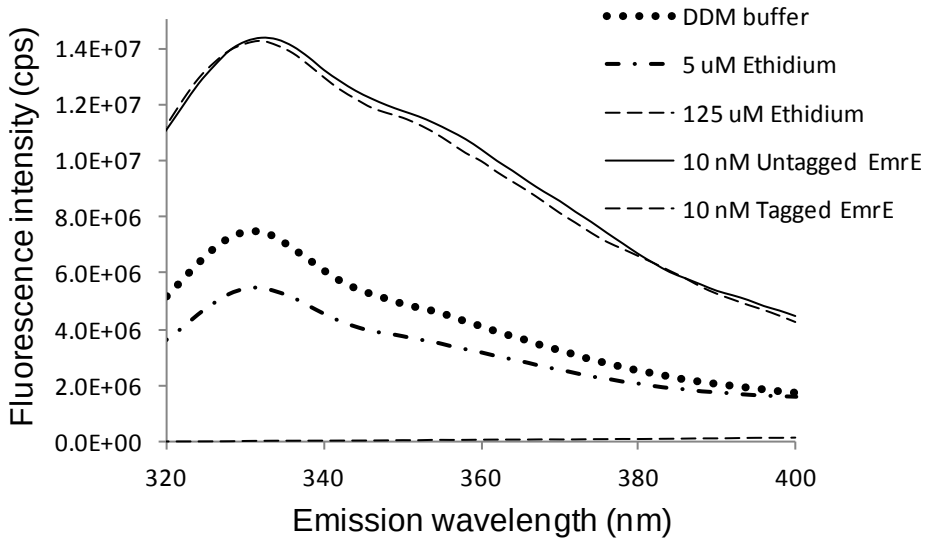

Figure 6.1: The baseline spectra (DDM buffer) displays emission when excited with 295 nm light. Addition of ligand (in this case, ethidium), decreases the emission intensity approaching 0 cps at 125 µM of ethidium. Spectra of 10 nM untagged and tagged EmrE before subtracting the baseline are included to show that they are above baseline levels. Each emission spectra were recorded through the S/R channel and at a slit-width of 10 nm for both excitation and emission.

7.2.2 Calculations and plotting of ligand binding curves

Some ligands also exhibited fluorescence in the emission range tested that overlapped with the EmrE emission spectra. To correct for this, a titration of a blank (DDM buffer without EmrE) with ligand was performed and the emission spectra were subtracted from the EmrE-ligand spectra at each ligand concentration.

Fluorescence quenching could not be monitored at the emission maxima (λ_{max}) of each ligand-titrated protein spectrum as the λ_{max} was variable for different ligand concentrations. As such, the λ_{max} corresponding to protein spectrum collected at each ligand concentration were averaged together and this wavelength (λ_{avg}) was selected to monitor all fluorescence intensity changes. For each ligand titration, the fluorescence intensity at λ_{avg} was recorded. A percent change in fluorescence intensity was calculated relative to an EmrE sample lacking the ligand. The percent quenching was plotted against ligand concentration and a one-site total binding curve was fitted using Graphpad Prism 5 software. The equation used for curve fitting was as follows:

$$\text{Specific binding} = B_{max} * [\text{ligand}] / (K_d + [\text{ligand}]) \quad (2)$$

Where the total fluorescence intensity change is a measure of specific binding, B_{max} is the maximum specific one-site binding, [ligand] is the ligand concentration.

7.2.3 Ligand binding

Binding was observed of both EmrE with all 3 of the ligands tested. The residual plots in figure 6.3 corresponding to each ligand binding curve show how close the curve

fitting algorithm was with respect to the individual data points. Deviations from the one-site specific binding model were similar between untagged and tagged EmrE due to overlaps of error bars (figure 6.3). Thus, both types of EmrE could be compared using this binding model. K_d and B_{max} values are listed in table 6.2. According to the overlap of the 95% confidence intervals the B_{max} of the ethidium and cetylpyridinium were likely to be similar between both types of EmrE whereas the methyl viologen titration was likely to be different. By the same rationale, only the K_d values for the ethidium titration were likely to be different between untagged and tagged EmrE. In the case of ethidium binding, tagged EmrE had a K_d of 86 ± 22 and untagged had a K_d of 18 ± 2. Due to the smaller dissociation constant, untagged EmrE had nearly a 4-5 times stronger binding interaction than tagged EmrE with ethidium. Similarly, untagged EmrE also binds methyl viologen tighter than tagged EmrE. However, there was some ambiguity for the methyl viologen K_d values where the confidence intervals shares a small overlap at 164 µM (table 6.2).

Table 6.2: Summary of EmrE-ligand binding values

	Ethidium		Methyl viologen		Cetylpyridinium	
	Untagged	Tagged	Untagged	Tagged	Untagged	Tagged
Bmax (% fluorescence intensity decrease)	120 ± 3	175 ± 26	106 ± 3	63 ± 4	69 ± 3	73 ± 3
Kd (μM)	18 ± 2	86 ± 22	139 ± 12	266 ± 51	57 ± 9	93 ± 12
	95% confidence interval					
Bmax (% fluorescence intensity decrease)	113 to 126	123 to 227	101 to 111	55 to 72	63 to 76	67 to 80
Kd (μM)	15 to 21	41 to 132	115 to 164	164 to 367	38 to 76	68 to 117

*± values indicate standard deviation. Each experiment was replicated 3 times with each replicate data set representing samples from different purifications.

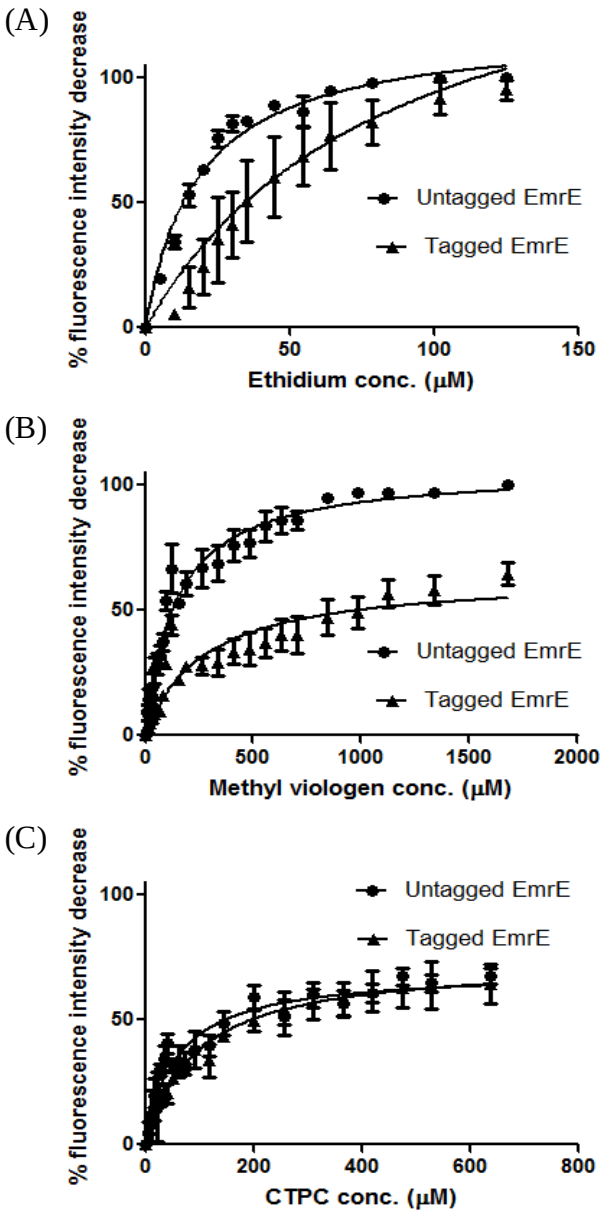

Figure 6.2: Binding curves of untagged and tagged EmrE with (A) ethidium bromide, (B) methyl viologen, and (C) cetylpyridinium chloride. Each data point represents a mean of 2-3 biological replicate data sets.

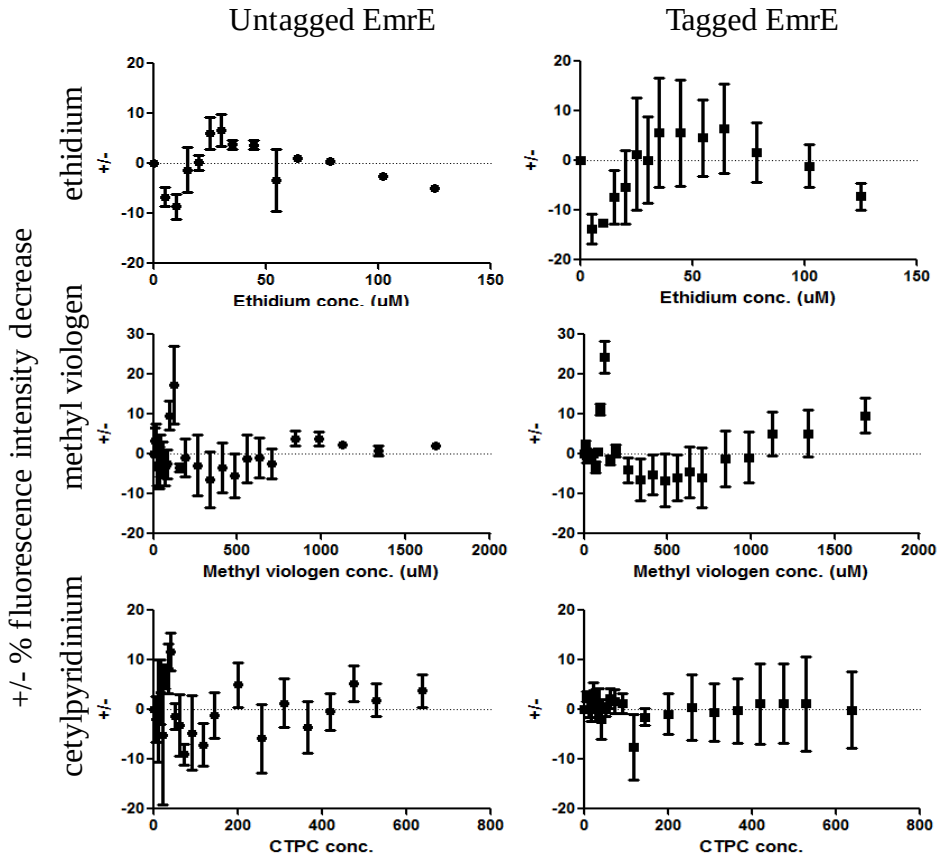

Figure 6.3: Residual plot showing how much the fitted ligand binding curves deviate from each data point.

7.3 Discussion

The binding site of EmrE is located within the transmembrane region and is largely based on the anionic-charged residue, Glu14 (Muth and Schuldiner, 2000). The p*K* of this residue was estimated to be 8.3-8.5 (Soskine *et al.,* 2004). The negative charge interacts with protons and the QCC substrate for facilitation of anti-port transport. In addition, Trp residues, such as Trp63 in EmrE can participate in a cation-pi interaction with protons (Dougherty, 1996). The fluorescence decrease during the ligand titrations were mainly due to this Trp63 in close proximity to the ligand. Mutation of the other tryptophans has little effect on the overall protein fluorescence (Elbaz *et al*., 2005). With this in mind, ligand affinity depends not only on the specific chemistry at the binding site, but also access to the binding site. A B_{max} near 100% fluorescence intensity decrease indicates binding of ligand to all EmrE molecules in solution. In the case of CTPC, the low saturation could be due to the surfactant nature of CTPC favoring the formation of micelles at higher concentrations. At these concentrations, the EmrE-CTPC interactions decrease due to a higher preference for the formation of micelles.

Similarly, the methyl viologen titration did not fully bind all of the tagged EmrE. Unlike CTPC, methyl viologen does not possess surfactant characteristics though the theme of binding site access can be maintained. Methyl viologen bound to all the untagged EmrE, but only a portion of tagged EmrE. Thus, a population of the tagged EmrE in solution was in a conformation which prevents binding (figure 6.4). From the fluorescence data in chapter 4 it was proposed that some population of tagged EmrE in the sample adopted a water-occluded state. This state could be stabilized by the tag or during the purification. Note that a lower effective binding population of tagged EmrE

does not change K_d, but the B_{max} is reached at lower titrant concentration. In contrast, untagged EmrE reached a higher B_{max} which may indicate that there are more binding sites available to bind methyl viologen. This means that either the method of purifying EmrE or the presence of a fusion tag affects the way EmrE binds ligand. Exposure of untagged EmrE to organic solvents during purification may release any binding-site occluded states by inducing a monomeric state (Winstone *et al*., 2005). Dissociation of the EmrE dimer can also remove any intermediate binding states. Reconstitution of untagged EmrE in the detergent, DDM, yields a sample that binds ligand in a relatively more uniform fashion. On the other hand, tagged EmrE samples purified in this study contain a mixture of binding and non-binding proteins. However, this difference was not observed with the ethidium titrations. Both untagged and tagged EmrE binding sites were saturated during the ethidium titration to comparable B_{max}. Ethidium and methyl viologen differ by charge and 3-dimensional structure. Methyl viologen contains 2 positive charges and has a "twisted" shape whereas ethidium only has 1 and has a planar shape. This implies that the binding site of tagged EmrE restricted access to methyl viologen based on its dual positive charge and relatively bulkier non-planar shape (figure 1.3).

With the exception of CTPC, the binding of ethidium and methyl viologen follow the same trend of binding affinity observed for untagged EmrE when analyzed by isothermal titration calorimetry (Sikora and Turner, 2005). Both types of EmrE have a higher binding affinity for ethidium over methyl viologen though overall, untagged EmrE displays a higher affinity for these ligands. Previous reports of K_d of tagged EmrE have been in the nano-molar range due to the nature of the binding assays (table 6.1). This made it difficult to compare with untagged EmrE K_d in the micro-molar range obtained

under different assaying conditions (table 6.1). For the conditions used in this study, untagged EmrE displayed a tighter binding to ethidium and methyl viologen than tagged EmrE while the CTPC affnities could not be conclusively distinguished.

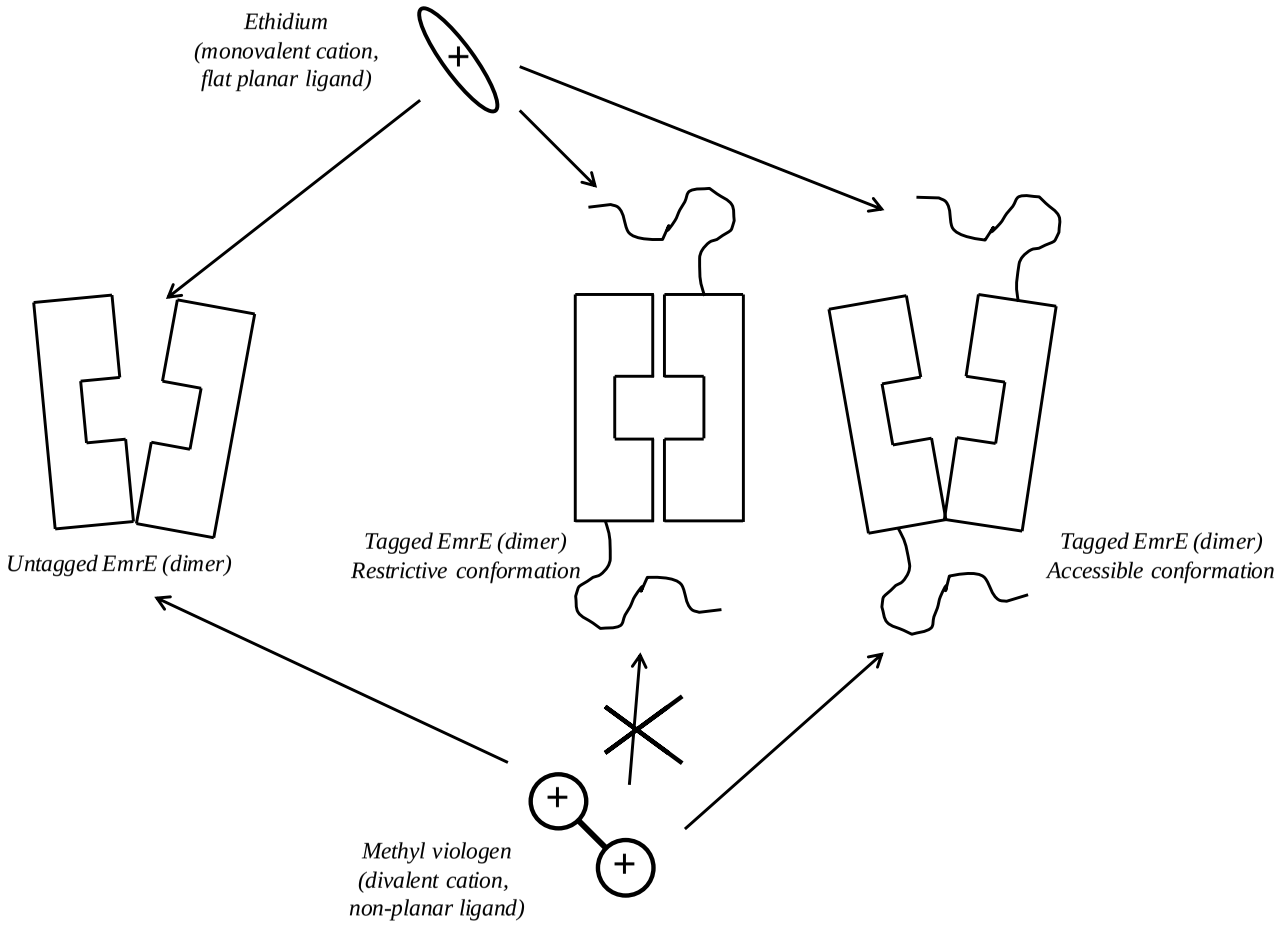

Figure 6.4: Representation of ethidium and methyl viologen binding to untagged and tagged EmrE. Both untagged and tagged EmrE bound ethidium. A population of tagged EmrE did not bind methyl viologen.

Chapter Eight: **Resistance assays**

8.1 Background

A simple functional assay was performed in vivo where only cell culture techniques were involved. Resistance of the host bacteria to QCC relies on the transport mechanism of EmrE. Transport involves the release of substrate as well as binding. In vitro conditions may cause misinterpretation of a protein's natural behaviour due to the solubilisation in a detergent buffer. In this assay, variables introduced by the purification conditions were intentionally excluded to directly examine the effect of the peptide tag on QCC transport by EmrE. The presence of a tag can disrupt transport through several means: occluding the binding site, preventing oligomerization, or influencing the topological state. Additionally, the transport dynamics could also be affected. Currently, EmrE is modelled as an asymmetric dimer that follows a single-site alternating access model (Fleishman et al., 1996; Henzler-Wildman, 2012). According to this model, the individual EmrE monomers interchange between 2 states, A and B. In an AB state, the active site of the dimer is exposed to one side of the lipid bilayer and upon binding or releasing ligand there is a conformational change into the BA state. Figure 7.1B diagrams the possible ways a peptide tag can interfere with transport. In an asymmetric dimer, the peptide tag can interfere with the initial access of the ligand as well as the release from the other side of the transporter. Dimerization can also be affected if the tag disrupts helix-helix interactions, thus preventing the formation of the functional EmrE unit. There are 6 negatively charged glutamates located in the tag and may bias the topology of EmrE according to the positive inside rule (von Heijne, 1989).

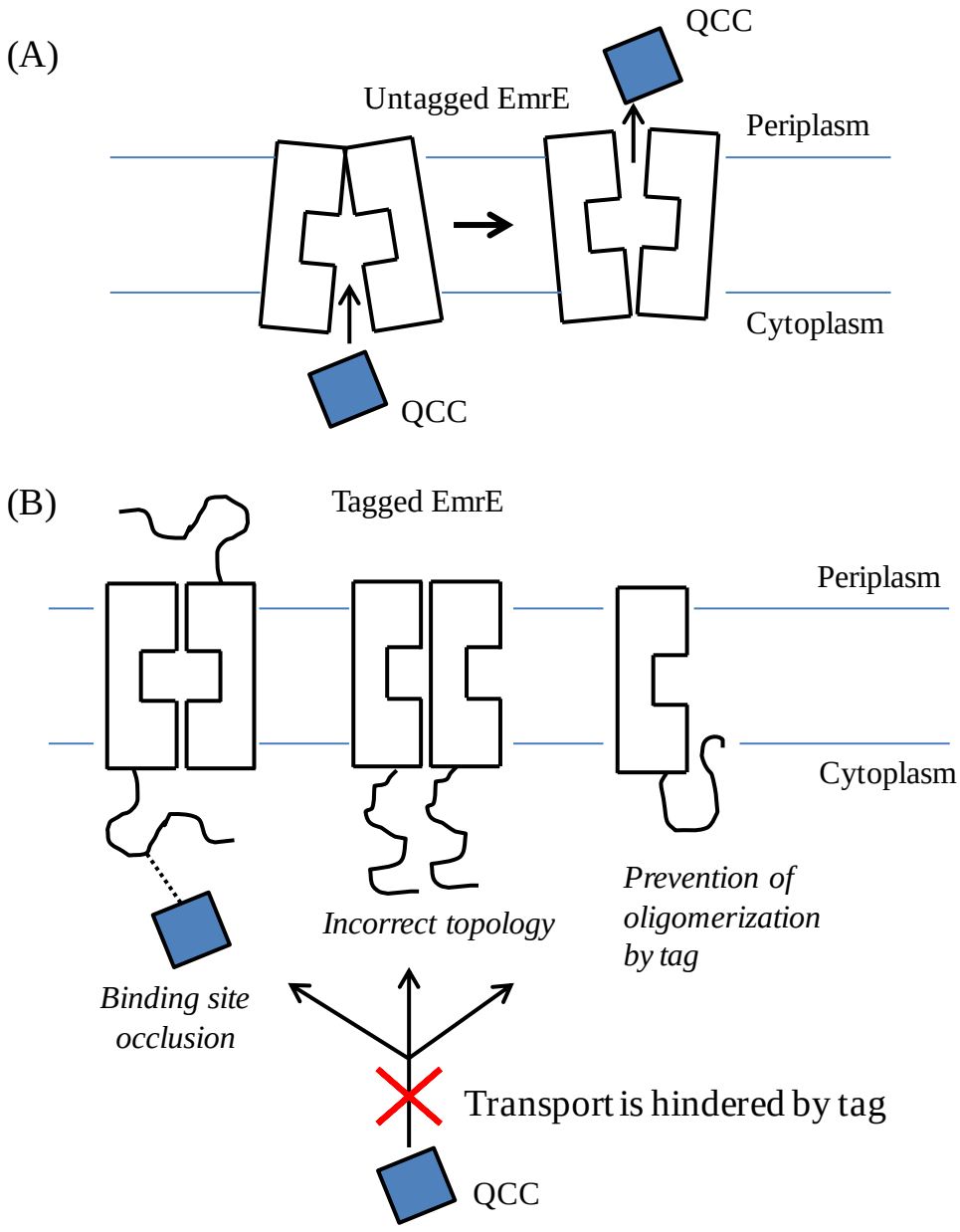

Figure 7.1: (A) QCC efflux by untagged EmrE. (B) Possible ways in which the peptide tag can interfere with QCC efflux for tagged EmrE.

8.2 Results

The endpoint measurement after 26 h of growth was plotted against QCC concentration (figure 7.2). Growth curves constructed from earlier time-points indicated that at 26 h, all cultures were at a stationary phase of growth (not shown). Untagged EmrE cultures displayed higher resistance than tagged EmrE cultures to ethidium at concentrations between 6 and 99 µM. Cultures containing either untagged or tagged e*mrE* plasmids had a reduced OD_{550} compared to cultures containing empty vector or no plasmid in the presence of up to 2.4 mM methyl viologen. In the presence of higher MV concentrations upwards of 2.4 mM, both untagged and tagged EmrE have cell densities equal to or greater than the control cultures. For all ranges of methyl viologen concentrations tested, untagged EmrE cultures had consistently higher cell densities than tagged EmrE cultures. All cultures grown in the presence of 7.2 µM up to 7.4 mM cetylpyridinium did not display any significant growth at all time-points measured.

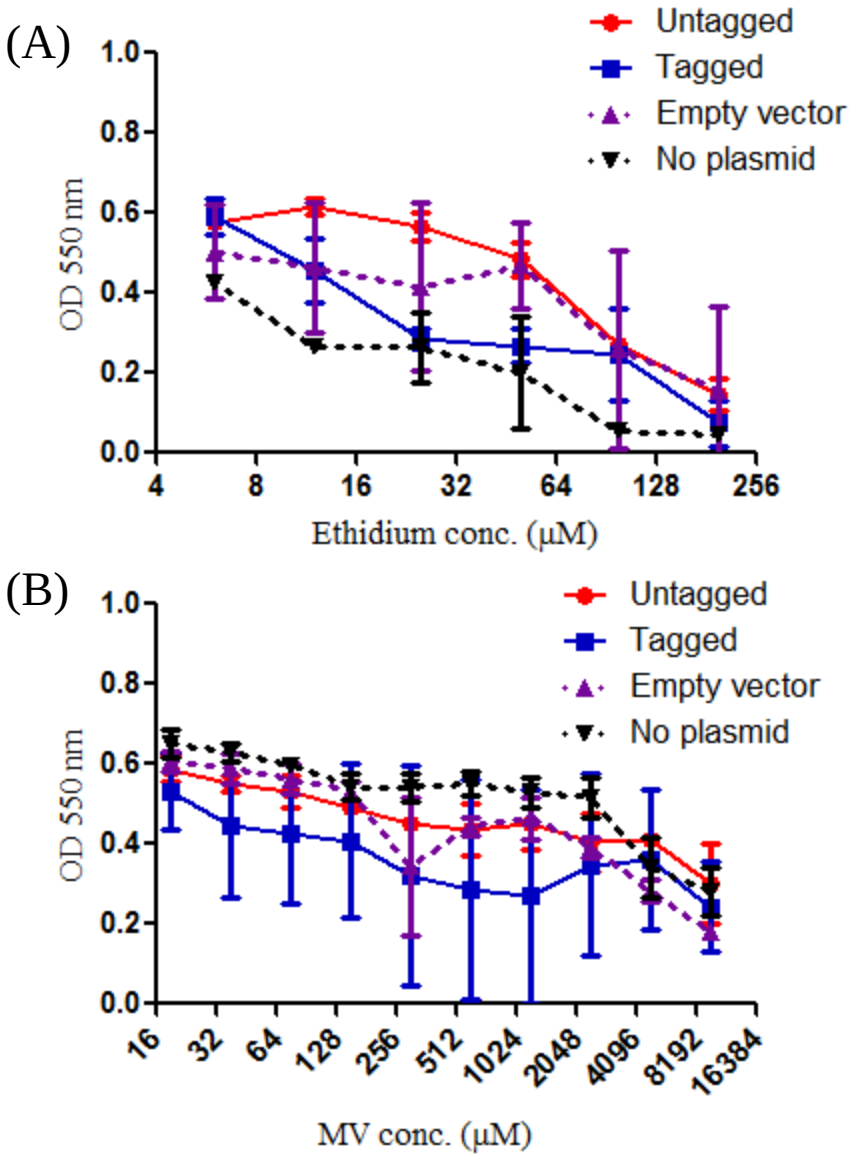

Figure 7.2: Cell culture optical densities recorded at 550 nm plotted against different concentrations of (A) ethidium or (B) methyl viologen present in the growth media. E. coli *cells containing either the untagged or tagged EmrE plasmids were compared to cells containing the non-EmrE-coding plasmid (empty vector) and cells without any plasmid added.*

8.3 Discussion

The natural substrates of EmrE are currently unknown. The known cytotoxic QCC that are resisted through transport by EmrE are not abundantly found in natural bacterial environments. Though QCC binding has been observed *in vitro*, QCC resistance conferred by EmrE may have varying degrees of effectiveness. Notably, CTPC was lethal at all concentrations tested in this study. Binding of CTPC *in vitro* has been previously observed in isothermal titration calorimetry experiments (Sikora and Turner, 2005). However, EmrE was not able to curb the toxicity of CTPC to cells in culture. As the structure of CTPC resembles an amphipathic detergent molecule, a resistance transport mechanism may not be effective. Detergents associate with membranes and disrupt them. As a result, it makes little difference which side of the membrane the drug is on. In contrast, EmrE was more effective in protecting cells from drugs that target intracellular content like ethidium and methyl viologen. Ethidium toxicity works in prokaryotes by binding DNA and inhibiting binding of enzymes required for replication whereas methyl viologen triggers the generation of reactive oxygen species causing oxidative stress. Cells contained untagged EmrE displayed better resistance to both of these compounds and hence, better transport.

Cultures containing the empty vector survived better than cultures that did not contain the plasmid. This is no surprise as the presence of the plasmid itself can increase cell viability in the presence of ethidium, a DNA binding dye. Binding of the dye to non-essential plasmid DNA can mitigate inhibition of essential gene expression. Tagged EmrE cultures reached a 26 h endpoint density between the empty vector and no plasmid cultures. The tagged EmrE plasmid itself is sufficient to explain the survivability over no-

plasmid cultures, but it was puzzling that the tagged EmrE protein itself was reducing the cell viability over cultures containing empty vector. It must be noted that the bacteria strain used in this study are not *emrE*-knockout strains. Chromosomally encoded EmrE can provide a basal level of resistance. An anti-synergistic effect can form between plasmid-encoded and chromosomally encoded EmrE. This has been termed the negative-dominance effect which occurs when an EmrE oligomer contains at least one non-functional monomer unit (Yerushalmi *et al.,* 1996; Rotem *et al.,* 2001). Thus, tagged EmrE can form non-functional oligomers with wild-type EmrE to reduce the efflux of ethidium. The basic functional unit of EmrE is likely an anti-parallel dimer (Morrison *et al*., 2012; Henzler-Wildman, 2012). In other words, the oligomer requires two different topological orientated EmrE to efflux QCC. Due to a single permanent positive charge on the *myc-His*$_6$ tag of tagged EmrE, the topology could be biased towards a single orientation. This arrangement can prevent the formation of the binding cavity. Thus, any pairings of tagged EmrE with itself or wild-type EmrE of the same topology will be non-functional. Occlusion of the binding site by the tag can also lead to the negative dominance effect. Half of an anti-parallel EmrE dimer is composed of 4 transmembrane helices. Tagged EmrE has a 27 amino acid-long peptide attached to one of these helices. This places the tag close to the binding cavity access site. The exact mechanism of dysfunction cannot be defined in the scope of this study. However, it is clear that the N-terminal *myc-his*$_6$ tag interferes with efflux-mediated ethidium resistance *in vivo*. A similar conclusion can be drawn for the MV resistance comparison. Untagged EmrE culture endpoint densities were consistently higher that tagged EmrE within the tested

range of MV concentrations. This indicates that the reduced resistance due to the tag was not limited to monovalent QCC.

Chapter Nine: **Conclusions**

The original objective of this thesis was to characterize differences in the structure and function of untagged and tagged EmrE. After the successful execution of each preparation, a sufficient amount of sample was obtained to carry out the biochemical and biophysical assays that followed. Specifically, the first aim was to characterize differences in structure and dynamics of EmrE using fluorescence. Functionality was then assessed through titrations with EmrE ligands to obtain binding constants. The final assay was performed *in vivo* to measure the effect of the affinity tag alone on the effect of transport. All of these assays provided valuable insight into the interactions of an affinity peptide tag with the transmembrane region of an integral membrane protein.

Initially, the tagged EmrE preparation was developed as an alternative method to the use of organic solvents to purify untagged EmrE. The affinity tag allowed for a convenient set-up that required only 2 chromatography steps and a gradual transfer of the membrane protein into DDM buffer, the buffer used for all the *in vitro* assays in this study. In contrast, the untagged EmrE purification required a multi-stepped organic extraction and delipidation step. Additionally, the reconstitution of the untagged EmrE into a detergent solution was not as efficient as insoluble sample was removed by centrifugation. In the end, the tagged EmrE preparation led to a more homogenous sample solution that did not scatter as much light between 240-260 nm (figure 3.4). Tagged EmrE yields were also at least 5 times higher. This translated to 5 times less time for growing and harvesting cell cultures (table 3.1).

The first structural difference was observed when the EmrE samples were selectively excited at 295 nm. The fluorescence emission spectrum provided clues as to where the tryptophan residues were located on the protein tertiary structure. Both untagged and tagged EmrE shared a λ_{max} at around 338 nm (figure 4.1). This value corresponded to the maxima of the Trp63 residue of EmrE (Elbaz *et al*., 2005). Trp63 has been mapped to the binding site of EmrE (Elbaz *et al.*, 2005. Sharoni *et al.*, 2005) and it would appear that both EmrE have a similarly hydrophobic binding site. However, a 328 nm emission peak exclusive to the tagged EmrE spectrum indicated a separate population of tryptophans in a relatively more hydrophobic environment. It was not known which of the 4 Trp in EmrE contributed to this emission. Regardless, the second peak was linked to a different conformation adopted by some of the tagged EmrE in the sample. Decreased fluorescence intensity of untagged EmrE was attributed to photo-reaction with chloroform (Ladner *et al*., 2004) rather than to any structural causes.

A red-edge excitation shift (REES) assay was performed to probe environmental dynamics surrounding the fluorophores in EmrE. Untagged EmrE was observed to have its Trp side-chains in a more dynamic environment. This was characterized by the "reverse-relaxation" phenomenon (figure 5.4) which can only occur if the timescale of emission is close to the timescale of solvent reorientation (Nemkovich *et al*., 1979; Lakowicz, 2006). The solvent re-orientation surrounding Trp residues in tagged EmrE were in comparison much slower (figure 5.2). Overall, these results can be evaluated in terms of helix packing or displacement of solvent molecules by the affinity tag in tagged EmrE. The tighter packing of tagged EmrE can restrict solvent reorientation. As a red-shifted emission for both EmrE is observed at or is above 295 nm, it can be assumed that

the effect is related to Trp residues. Together with the fluorescence spectral data, this places the tryptophans of tagged EmrE in a more hydrophobic environment as well as a more spatially compact environment.

Tertiary arrangements of the transmembrane helices and oligomerization form the binding site of EmrE (Sharoni *et al.,* 2005). Subtle differences in the angular positioning can place side-chains responsible for binding closer or further away from a ligand. Both EmrE have a higher affinity to ethidium than to methyl viologen indicating the preference for a singly positive charged ligand (figure 6.2). Notably, a population of tagged EmrE do not even bind methyl viologen as evident from the saturation at lower methyl viologen concentrations. Surprisingly, ethidium was able to by-pass the binding site occlusion. This could be due to the nature of tagged EmrE binding site interacting more favorably with the relatively more hydrophobic ethidium. Tagged EmrE also has a reduced affinity to both ethidium and methyl violgen when compared with untagged EmrE. The conformation of untagged EmrE may allow for a more flexible binding site access. This could also explain how the untagged form reaches saturation with both ethidium and MV due to less occlusion and/or ability to accommodate more hydrophilic molecules.

Lastly, functional transport was prevented by the tag *in vivo* (figure 7.2). Factors such as solubilisation conditions and side-reactions with organic solvents could not have produced this result. By itself, the tag alone was enough to inhibit transport activity. Untagged EmrE cultures displayed a higher resistance to both ethidium and methyl viologen than the tagged EmrE cultures. Furthermore, pairings of tagged EmrE with chromosomally encoded tagged EmrE demonstrated the negative-dominance effect (Yerushalmi *et al*., 1996; Rotem *et al.,* 2001). This was apparent when tagged EmrE

cultures displayed less resistance to ethidium than empty vector cultures that only contained chromosomally encoded EmrE.

Overall, the His_6 tag can influence the conformation within transmembrane alpha-helices. These results show that despite having a more efficient purification and solubilisation, affinity-tagged integral membrane proteins may lose structure and functionality.

Chapter Ten: **Bibliography**

Arora, A. and Tamm L. K. (2001) Biophysical approaches to membrane protein structure determination. Current Opinion in Structural Biology **11**, 540-547.

Awasthi, Y. C., Chuang, T. F., Keenan, T. W. and Crane, F. L. (1971) Tightly bound cardiolipin in cytochrome oxidase. Biochimica et Biophysica Acta (BBA) - Bioenergetics **226**, 42–52.

Basting, D., Lorch, M., Lehner, I. and Glaubitz, C. (2008) Transport cycle intermediate in small multidrug resistance protein is revealed by substrate fluorescence. FASEB journal : official publication of the Federation of American Societies for Experimental Biology **22**, 365–373.

Bay, D. C., Rommens, K. L. and Turner, R. J. (2008) Small multidrug resistance proteins: a multidrug transporter family that continues to grow. Biochimica et biophysica acta **1778**, 1814–1838.

Butler, P. J. G., Ubarretxena-Belandia, I., Warne, T. and Tate, C. G. (2004) The Escherichia coli multidrug transporter EmrE is a dimer in the detergent-solubilised state. Journal of molecular biology **340**, 797–808.

Chen, Y.-J., Pornillos, O., Lieu, S., Ma, C., Chen, A. P. and Chang, G. (2007) X-ray structure of EmrE supports dual topology model. Proceedings of the National Academy of Sciences of the United States of America **104**, 18999–19004.

Choi, J. H. and Lee, S. Y. (2004) Secretory and extracellular production of recombinant proteins using Escherichia coli. Applied microbiology and biotechnology **64**, 625–635.

De Boer, H. A., Comstock, L. J., Vasser, M. (1983) The tac promoter: A functional hybrid derived from the *trp* and *lac* promoters. Proceedings of the National Academy of Sciences of the United States of America **80**, 21–25.

Dougherty, D. A. (1996) Cation-pi interactions in chemistry and biology: a new view of benzene, Phe, Tyr, and Trp. Science (New York, N.Y.) **271**, 163–168.

Elbaz, Y., Tayer, N., Steinfels, E., Steiner-Mordoch, S., Schuldiner, S. (2005) Substrate-Induced Tryptophan Fluorescence Changes in EmrE, the Smallest Ion-Coupled Multidrug Transporter. Biochemistry **44**, 7369-7377.

Federkeil, S. L., Winstone, T. L., Jickling, G. and Turner, R. J. (2003) Examination of EmrE conformational differences in various membrane mimetic environments. Biochemistry and Cell Biology **81**, 61–70.

Fleishman, S. J., Harrington, S. E., Enosh, A., Halperin, D., Tate, C. G. and Ben-Tal, N. (2006) Quasi-symmetry in the cryo-EM structure of EmrE provides the key to modeling its transmembrane domain. Journal of molecular biology **364**, 54–67.

Fürste, J. P., Pansegrau, W., Frank, R., Blöcker, H., Scholz, P., Bagdasarian, M. and Lanka, E. (1986) Molecular cloning of the plasmid RP4 primase region in a multi-host-range tacP expression vector. Gene **48**, 119–131.

Gill, S. C. and von Hippel, P. H. (1989) Calculation of protein extinction coefficients from amino acid sequence data. Analytical biochemistry **182**, 319–326.

Grinius, L. L. and Goldberg, E. B. (1994) Bacterial multidrug resistance is due to a single membrane protein which functions as a drug pump. The Journal of biological chemistry **269**, 29998–30004.

Heijne, G. Von. (1992) Membrane Protein Structure Prediction: Hydrophobicity Analysis and the Positive-inside Rule. Journal of Molecular Biology **225**, 487-494.

Henzler-Wildman, K. (2012) Analyzing conformational changes in the transport cycle of EmrE. Current opinion in structural biology, Elsevier Ltd **22**, 38–43.

Jardetsky, O. (1966) Simple Allosteric Model for Membrane Pumps. Nature **211**, 969–970.

Ksenzenko, S. M. and Brusilow, W. S. A. (1993) Protein-Lipid Interactions of the Proteolipid c Subunit of the Escherichia coli Proton-Translocating Adenosinetriphosphatase. Archives of biochemistry and biophysics **305**, 78–83.

Ladner, C. L., Yang, J., Turner, R. J. and Edwards, R. a. (2004) Visible fluorescent detection of proteins in polyacrylamide gels without staining. Analytical biochemistry **326**, 13–20.

le Maire, M., Champeil, P. and Moller, J. V. (2000) Interaction of membrane proteins and lipids with solubilizing detergents. Biochimica et biophysica acta **1508**, 86–111.

Lee, A. G. (2004) How lipids affect the activities of integral membrane proteins. Biochimica et biophysica acta **1666**, 62–87.

Lehner, I., Basting, D., Meyer, B., Haase, W., Manolikas, T., Kaiser, C., Karas, M. and Glaubitz, C. (2008) The key residue for substrate transport (Glu14) in the EmrE dimer is asymmetric. The Journal of biological chemistry **283**, 3281–3288.

Loll, P. J. (2003) Membrane protein structural biology: the high throughput challenge. Journal of Structural Biology **142**, 144–153.

Ma, C. and Chang, G. (2004) Structure of the multidrug resistance efflux transporter EmrE from Escherichia coli. Proceedings of the National Academy of Sciences of the United States of America **101**, 2852–2857.

Markwell, M. K., Haas, S. M. and Tolbert, N. E. (1978) Determination of the Lowry Procedure to Simplify Protein in Membrane and Lipoprotein **210**, 206–210.

Miller, D., Charalambous, K., Rotem, D., Schuldiner, S., Curnow, P. and Booth, P. J. (2009) In vitro unfolding and refolding of the small multidrug transporter EmrE. Journal of molecular biology, Elsevier B.V. **393**, 815–832.

Miroux, B. and Walker, J. E. (1996) Over-production of proteins in Escherichia coli: mutant hosts that allow synthesis of some membrane proteins and globular proteins at high levels. Journal of molecular biology **260**, 289–298.

Mori, H. and Ito, K. (2001) The Sec protein-translocation pathway. Trends in Microbiology **9**, 494–500.

Morrison, E. a, DeKoster, G. T., Dutta, S., Vafabakhsh, R., Clarkson, M. W., Bahl, A., Kern, D., Ha, T. and Henzler-Wildman, K. A. (2012) Antiparallel EmrE exports drugs by exchanging between asymmetric structures. Nature, Nature Publishing Group **481**, 45–50.

Muth, T. R. and Schuldiner, S. (2000) A membrane-embedded glutamate is required for ligand binding to the multidrug transporter EmrE. The EMBO journal **19**, 234–240.

Nemkovich, N. A., Matseiko, V. I., Rubinov, A. N. and Tomin, V. I. (1979) Intermolecular orientational “upward” relaxation in viscous solutions of organic compounds. Pis’ma Zh. Eksp. Teor. Fiz. **29**, 780–783.

Paulsen, I. T., Skurray, R. a, Tam, R., Saier, M. H., Turner, R. J., Weiner, J. H., Goldberg, E. B. and Grinius, L. L. (1996) The SMR family: a novel family of multidrug efflux proteins involved with the efflux of lipophilic drugs. Molecular microbiology **19**, 1167–1175.

Popot, J. L., Gerchman, S. E. and Engelman, D. M. (1987) Refolding of bacteriorhodopsin in lipid bilayers. A thermodynamically controlled two-stage process. Journal of molecular biology **198**, 655–676.

Porath, J., Carlsson, J., Olsson, I. and Belfrage, G. (1975) Metal chelate affinity chromatography, a new approach to protein fractionation. Nature **258**, 598–599.

Rigaud, J.-L. and Lévy, D. (2003) Reconstitution of membrane proteins into liposomes. Methods in enzymology **372**, 65–86.

Rolfe, M. D., Rice, C. J., Lucchini, S., Pin, C., Thompson, A., Cameron, A. D. S., Alston, M., Stringer, M. F., Betts, R. P., Baranyi, J., et al. (2012) Lag phase is a distinct growth phase that prepares bacteria for exponential growth and involves transient metal accumulation. Journal of bacteriology **194**, 686–701.

Rotem, D., Sal-man, N. and Schuldiner, S. (2001) In vitro monomer swapping in EmrE, a multidrug transporter from Escherichia coli, reveals that the oligomer is the functional unit. The Journal of biological chemistry **276**, 48243–48249.

Rotem, D., Steiner-Mordoch, S. and Schuldiner, S. (2006) Identification of tyrosine residues critical for the function of an ion-coupled multidrug transporter. The Journal of biological chemistry **281**, 18715–18722.

Rudolph, R. and Lilie, H. (1996) In vitro folding of inclusion body proteins. The FASEB journal **10**, 49-56.

Samuelson, J. C., Chen, M., Jiang, F., Möller, I., Wiedmann, M., Kuhn, a, Phillips, G. J. and Dalbey, R. E. (2000) YidC mediates membrane protein insertion in bacteria. Nature **406**, 637–641.

Schägger, H. (2006) Tricine-SDS-PAGE. Nature protocols **1**, 16–22.

Schleiff, E. and Soll, J. (2005) Membrane protein insertion: mixing eukaryotic and prokaryotic concepts. EMBO reports **6**, 1023–1027.

Schuldiner, S., Granot, D., Mordoch, S. S., Ninio, S., Rotem, D., Soskin, M., Tate, C. G. and Yerushalmi, H. (2001) Small is mighty: EmrE, a multidrug transporter as an experimental paradigm. News in physiological sciences **16**, 130–134.

Schuldiner, S., Lebendiker, M. and Yerushalmi, H. (1997) EmrE, the smallest ion-coupled transporter, provides a unique paradigm for structure-function studies. The Journal of experimental biology **200**, 335–341.

Schwaiger, M., Lebendiker, M., Yerushalmi, H., Coles, M., Gröger, a, Schwarz, C., Schuldiner, S. and Kessler, H. (1998) NMR investigation of the multidrug transporter EmrE, an integral membrane protein. European journal of biochemistry / FEBS **254**, 610–619.

Seddon, A. M., Curnow, P. and Booth, P. J. (2004) Membrane proteins, lipids and detergents: not just a soap opera. Biochimica et biophysica acta **1666**, 105–117.

Sharoni, M., Steiner-Mordoch, S. and Schuldiner, S. (2005) Exploring the binding domain of EmrE, the smallest multidrug transporter. The Journal of biological chemistry **280**, 32849–32855.

Sikora, C. W. and Turner, R. J. (2005) Investigation of ligand binding to the multidrug resistance protein EmrE by isothermal titration calorimetry. Biophysical journal, Elsevier **88**, 475–482.

Soskine, M., Adam, Y. and Schuldiner, S. (2004) Direct evidence for substrate-induced proton release in detergent-solubilized EmrE, a multidrug transporter. The Journal of biological chemistry **279**, 9951–9955.

Soskine, M., Steiner-Mordoch, S. and Schuldiner, S. (2002) Crosslinking of membrane-embedded cysteines reveals contact points in the EmrE oligomer. Proceedings of the National Academy of Sciences of the United States of America **99**, 12043–12048.

Tabor, S. and Richardson, C. C. (1985) A bacteriophage T7 RNA polymerase/promoter system for controlled exclusive expression of specific genes. Proceedings of the Natural Academy of Sciences of the United States of America **82**, 1074–1078.

Tate, C. G., Kunji, E. R., Lebendiker, M. and Schuldiner, S. (2001) The projection structure of EmrE, a proton-linked multidrug transporter from Escherichia coli, at 7 A resolution. The EMBO journal **20**, 77–81.

Tate, C. G., Ubarretxena-Belandia, I. and Baldwin, J. M. (2003) Conformational Changes in the Multidrug Transporter EmrE Associated with Substrate Binding. Journal of Molecular Biology **332**, 229–242.

Terpe, K. (2003) Overview of tag protein fusions: from molecular and biochemical fundamentals to commercial systems. Applied microbiology and biotechnology **60**, 523–533.

Tsumoto, K., Ejima, D., Kumagai, I. and Arakawa, T. (2003) Practical considerations in refolding proteins from inclusion bodies. Protein Expression and Purification **28**, 1–8.

Turner, R. J., Taylor, D. E. and Weiner, J. H. (1997) Expression of Escherichia coli TehA gives resistance to antiseptics and disinfectants similar to that conferred by multidrug resistance efflux pumps. Antimicrobial agents and chemotherapy **41**, 440–444.

Ubarretxena-Belandia, I., Baldwin, J. M., Schuldiner, S. and Tate, C. G. (2003) Three-dimensional structure of the bacterial multidrug transporter EmrE shows it is an asymmetric homodimer. The EMBO journal **22**, 6175–6181.

Wagner, S., Bader, M. L., Drew, D. and de Gier, J.-W. (2006) Rationalizing membrane protein overexpression. Trends in biotechnology **24**, 364–371.

Wallin, E. and von Heijne, G. (1998) Genome-wide analysis of integral membrane proteins from eubacterial, archaean, and eukaryotic organisms. Protein science **7**, 1029–1038.

White, S. H. and Wimley, W. C. (1999) Membrane protein folding and stability: physical principles. Annual review of biophysics and biomolecular structure **28**, 319–365.

Winstone, T. L., Duncalf, K. a and Turner, R. J. (2002) Optimization of expression and the purification by organic extraction of the integral membrane protein EmrE. Protein expression and purification **26**, 111–121.

Winstone, T. L., Jidenko, M., Ebel, C., Duncalf, K. A. and Turner, R. J. (2005) Organic solvent extracted EmrE solubilized in dodecyl maltoside is monomeric and binds drug ligand. Biochemical and biophysical research communications **327**, 437–445.

Wu, J. and Filutowicz, M. (1999) Hexahistidine (His6)-tag dependent protein dimerization: A cautionary tale. Acta Biochimica Polonica **46**, 591–599.

Yerushalmi, H., Lebendiker, M. and Schuldiner, S. (1996) Negative dominance studies demonstrate the oligomeric structure of EmrE, a multidrug antiporter from Escherichia coli. The Journal of biological chemistry **271**, 31044–31048.

Yerushalmi, H., Lebendiker, M. and Schuldiner, S. (1995) EmrE, an Escherichia coli 12-kDa Multidrug Transporter, Exchanges Toxic Cations and H+ and Is Soluble in Organic Solvents. The Journal of biological chemistry **270**, 6856–6863.